UNITED NATIONS UNIVERSITY

UNU-GTP

ORKUSTOFNUN

Meyjarauga hot spring, Hveravellir, Kjölur, Central Iceland

Kennedy Mativo Kamunya

δD AND $\delta^{18}O$ SYSTEMATICS IN GEOTHERMAL FLUIDS, OLKARIA GEOTHERMAL SYSTEM, KENYA

Report 4
November 2018

UNITED NATIONS UNIVERSITY
UNU-GTP
Geothermal Training Programme

Orkustofnun, Grensasvegur 9,
IS-108 Reykjavik, Iceland

Reports 2018
Number 4

δD AND $\delta^{18}O$ SYSTEMATICS IN GEOTHERMAL FLUIDS, OLKARIA GEOTHERMAL SYSTEM, KENYA

MSc thesis
School of Engineering and Natural Sciences
Faculty of Earth Sciences
University of Iceland

by

Kennedy Mativo Kamunya
Kenya Electricity Generating Company, Ltd.
Olkaria Geothermal Project
P.O. Box 785-20117 Naivasha,
KENYA
kkamunya@kengen.co.ke

United Nations University
Geothermal Training Programme
Reykjavík, Iceland
Published in November 2018

ISBN 978-9979-68-483-1 (PRINT)
ISBN 978-9979-68-484-8 (PDF)
ISSN 1670-7427

This MSc thesis has also been published in May 2018 by the
School of Engineering and Natural Sciences, Faculty of Earth Sciences
University of Iceland

INTRODUCTION

The Geothermal Training Programme of the United Nations University (UNU) has operated in Iceland since 1979 with six-month annual courses for professionals from developing countries. The aim is to assist developing countries with significant geothermal potential to build up groups of specialists that cover most aspects of geothermal exploration and development. During 1979-2018, 694 scientists and engineers from 61 developing countries have completed the six month courses, or similar. They have come from Africa (39%), Asia (35%), Latin America (14%), Europe (11%), and Oceania (1%). There is a steady flow of requests from all over the world for the six-month training and we can only meet a portion of the requests. Most of the trainees are awarded UNU Fellowships financed by the Government of Iceland.

Candidates for the six-month specialized training must have at least a BSc degree and a minimum of one-year practical experience in geothermal work in their home countries prior to the training. Many of our trainees have already completed their MSc or PhD degrees when they come to Iceland, but many excellent students with only BSc degrees have made requests to come again to Iceland for a higher academic degree. From 1999, UNU Fellows have also been given the chance to continue their studies and study for MSc degrees in geothermal science or engineering in co-operation with the University of Iceland. An agreement to this effect was signed with the University of Iceland. A similar agreement was also signed with Reykjavik University in 2013. The six-month studies at the UNU Geothermal Training Programme form a part of the graduate programme.

It is a pleasure to introduce the 60th UNU Fellow to complete the MSc studies under a UNU-GTP Fellowship. Kennedy Mativo Kamunya, a Geochemist from the Kenya Electricity Generating Company, Ltd. - KenGen in Kenya, completed the six-month specialized training in *Chemistry of Thermal Fluids* at UNU Geothermal Training Programme in October 2013. His research report was entitled: *Scaling potential during production in Hverahlíd field, Hengill high-temperature geothermal area, SW-Iceland.* After three years of geothermal work for KenGen at the Olkaria geothermal field in Kenya, he came back to Iceland for MSc studies at the School of Engineering and Natural Sciences, Faculty of Earth Sciences, University of Iceland in August 2016. In April 2018, he defended his *MSc thesis* in *Chemistry of Thermal Fluids* presented here, entitled: *δD and $\delta^{18}O$ systematics in geothermal fluids, Olkaria geothermal system, Kenya*. His studies in Iceland were financed by the Government of Iceland through a UNU-GTP Fellowship from the UNU Geothermal Training Programme. We congratulate Kennedy on the achievements and wish him all the best for the future. We thank the School of Engineering and Natural Sciences, Faculty of Earth Sciences, University of Iceland for the co-operation, and his supervisors for the dedication.

Finally, I would like to mention that Kennedy's MSc thesis with the figures in colour is available for downloading on our website *www.unugtp.is*, under publications.

With warmest greetings from Iceland,

Lúdvík S. Georgsson, Director
United Nations University
Geothermal Training Programme

ACKNOWLEDGEMENTS

I want to thank the United Nations University Geothermal Training Programme (UNU-GTP) and the Government of Iceland for awarding me a scholarship to study for the Master of Science degree at the University of Iceland. I want to thank the entire staff of UNU-GTP: the Director; Lúdvík S. Georgsson, Deputy director; Ingimar G. Haraldsson, Málfrídur Ómarsdóttir, Markús Andri Gordon and Thórhildur Ísberg for their support and ensuring a comfortable stay in Iceland during the course of my studies. I want to thank Kenya Electricity Generating Company (KenGen) for the support and granting me leave to pursue my studies.

I want to thank my supervisor Andri Stefánsson for his teaching, guidance and input throughout the course of this Master's thesis. I also want to thank Rósa Ólafsdóttir, Ríkey Kjartansdóttir and Jóhann Gunnarsson Robin from the University of Iceland for their assistance in analysis of the samples and data processing. I would like to thank the Geochemistry team in KenGen Olkaria for their help in collection of the samples.

Lastly, I give thanks to my family for their support, especially my mother for her prayers and her constantly checking up on me when I became too quiet

DEDICATION

This MSc thesis is dedicated to my late grandfather, Johnson Katumo Mutunga. For his recognition of the importance of education and striving to educate his children. This set a tradition that carries to this day

ABSTRACT

The δD and $\delta^{18}O$ systematics of geothermal fluids, Olkaria Kenya, were studied. Samples were collected from well discharges, both liquid and vapour phases collected at the same temperature and pressure, and analysed for major elemental and δD and $\delta^{18}O$ composition. The measured discharge fluids ranged in δD and $\delta^{18}O$ composition from -3.7 to +16.1‰ and -1.45 to +3.18‰, respectively. From these data, the reservoir chemical and isotope composition was reconstructed with δD and $\delta^{18}O$ ratios from -2.1 to +14.6‰ and -0.84 to +2.61‰, respectively. According to boiling modelling, large δD and $\delta^{18}O$ fractionations can occur from the reservoir to sampling at surface, and these changes exceed the range of observed δD and $\delta^{18}O$ variability for fluids. Accurate reconstruction of reservoir and source δD and $\delta^{18}O$ values requires, therefore, careful sampling, analysis and geochemical and isotope modelling. Based on the composition of the reservoir δD and $\delta^{18}O$ and the local rainwater, surface water, lake water and non-thermal groundwater, and consideration of total geothermal fluid discharge and annual precipitation, it is concluded that the geothermal reservoir fluids at Olkaria are predominantly meteoric origin locally and from the surrounding mountains. Upon water-rock interaction, the geothermal waters are further modified, shifting the $\delta^{18}O$ ratios to higher values.

TABLE OF CONTENTS

LIST OF FIGURES

Page

LIST OF TABLES

1. INTRODUCTION

Following the pioneering work of Craig, (1963, 1961) on δD and $\delta^{18}O$ isotope systematics of geothermal water, it is generally accepted today that geothermal water in geothermal systems originates from meteoric and sea water sources, or mixtures thereof, usually with minor contribution from magmatic sources (e.g., Arnórsson et al., 2007).

Commonly, the δD and $\delta^{18}O$ values of geothermal reservoir water show similar characteristics as the source water, typically being the local water of various origin. However, sometimes the δD and $\delta^{18}O$ values of the geothermal fluids differ from the local water, and such trends have usually been interpreted in terms of groundwater flow and ancient water reservoirs (e.g., Árnason, 1977; Pope et al., 2014; Stefánsson et al., 2017). However, water is a reactive component and its isotope composition can be modified by various processes occurring in geothermal systems. Water-rock interaction may change the $\delta^{18}O$ value of the bulk water through isotopic exchange with oxygen in the rocks (e.g., Truesdell and Hulston, 1980). In addition, the formation of alteration minerals and fractionation between the various minerals and the fluid may further change the δD and $\delta^{18}O$ values of the system. Similarly, boiling and formation of steam and liquid may result in fractionation of δD and $\delta^{18}O$ between the two fluid phases (e.g., Pope et al., 2016).

Several isotope studies have been carried out for the Olkaria geothermal system, Kenya, with the primary aim of tracing the origin of the geothermal fluids. The studies involved stable isotopes analyses of surface waters, (rivers, ground water, lakes and rainwater) geothermal well discharges and fumaroles (e.g., Allen and Darling, 1987; Allen et al., 1989; Clarke et al., 1990; Ojiambo and Lyons, 1993; Karingithi, 2000; Nkapiani, 2014; Owens et al., 2015). From these studies, it has been concluded that the geothermal water at Olkaria originates from meteoric recharge from the east and west flanks of the rift valley ($\delta^{18}O$ = -4.6 and δD = -28) and Lake Naivasha ($\delta^{18}O$ = +6.6 ‰ and δD = +36‰). Ojiambo and Lyons, (1993), suggested a possible third water source arguing that to produce the isotope composition of the geothermal water discharged in Olkaria, with isotope values of up to $\delta^{18}O$ = +5.3 and δD = +30.31, it would require 40-70% of Lake Naivasha water mixing with water from the flanks of the rift valley. Such an inflow would cool the reservoir substantially. A recent study in the west Olkaria field (Olkaria III) (Owens et al., 2015) identified a two component mixture, with a meteoric component and a deep water component from Lake Naivasha with the lake water accounting for 30-40% of the geothermal water discharge to east of Olkaria III. From these studies, definitive endmember components have not been identified and the contribution of each to the geothermal fluids is still uncertain. Tritium dating of Olkaria geothermal water from OW-2 and OW-26 (Clarke et al., 1990) gave a value of 0.23 TU or an age of over 40 years, suggesting a much longer flow path of the geothermal water than is suggested for a Lake Naivasha source, which is 2 km away from the geothermal field.

The aim of this study was to investigate and revisit the δD and $\delta^{18}O$ systematics of the geothermal system at Olkaria in an attempt to define the sources of geothermal fluids within the system. As the δD and $\delta^{18}O$ compositions are very sensitive to sampling, particularly boiling and evaporation, a new dataset was collected with well-defined sampling setups for both phases, vapour and liquid, followed by an analysis of major element and isotope compositions. In order to define the δD and $\delta^{18}O$ compositions of the reservoir geothermal fluids, the effects of boiling were systematically studied and the results compared with surrounding non-thermal waters.

2. STUDY AREA

2.1 Geological setting of Olkaria

The Olkaria geothermal area, Kenya, is located in the Greater Olkaria volcanic complex associated with the East African Rift System (EARS) that extents over 6000 km from the Afar region in Northern Ethiopia to the Zambezi valley in Mozambique (Figure 1). The section of the EARS in Kenya to Northern Tanzania is up to 900 km long. It is strongly segmented into tectonic units of contrasting age, size and type. The north and south are 200-300 km long, 80-100 km wide splay faulted regions. Between the north and southern regions is the central rift also known as the Gregory east African rift valley. It is 450 km long and 60-70 km wide with a symmetrical graben in some parts (e.g., Baker et al., 1972; Baker 1986; Macdonald et al., 1994). Olkaria is in the southern part of the central sector.

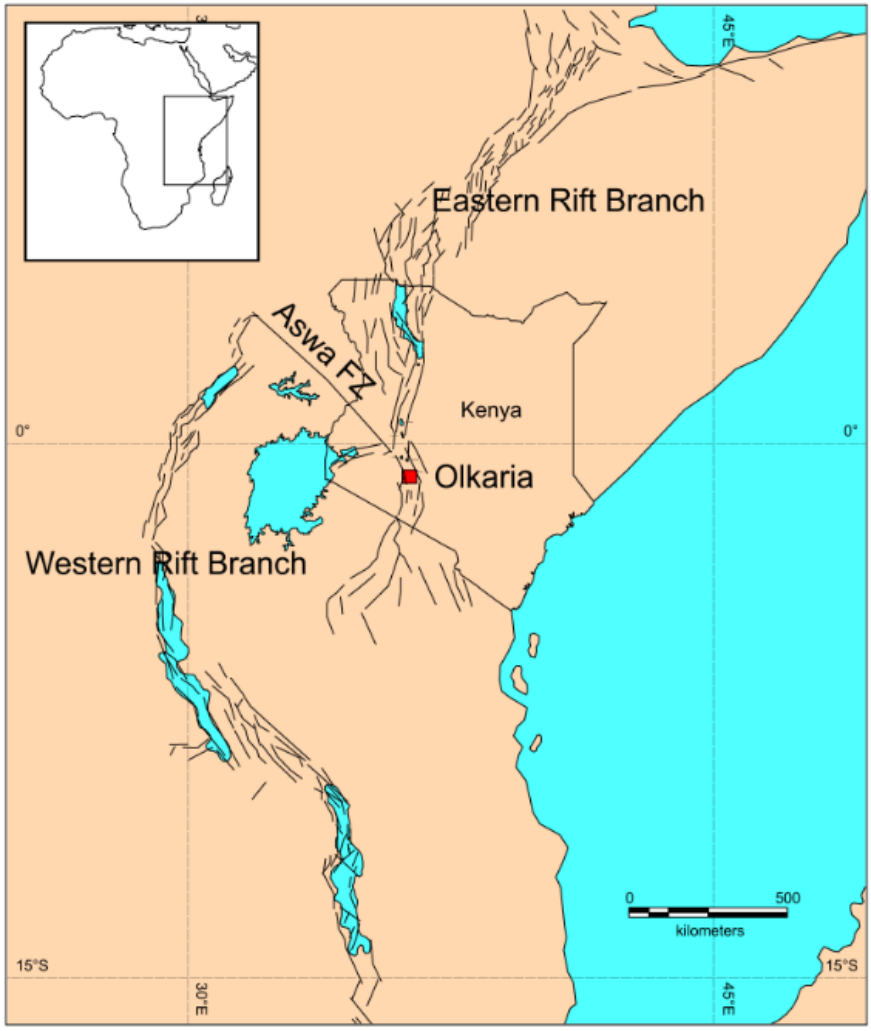

FIGURE 1: The East African Rift Valley system.
(Modified from Macgregor, 2015)

The EARS is a divergent plate boundary and is characterized by rifting tectonics and volcanism. In the rift section in Kenya, volcanism and rifting started in the Miocene (23 Ma) in the north and propagated to the south and reached the southern border with Tanzania about 5 Ma (e.g., Macdonald et al., 1994; Chorowicz, 2005). Flood volcanism characterized the initial stages of the formation of the EARS. Faulting throughout the history of the rift culminated in the formation of a step faulted graben and volcanism was gradually confined to the floor of the graben in the Quaternary period. The volcanism in the EARS in Kenya is bimodal and is composed of mainly basaltic and silicic rocks. The basaltic group includes alkali basalts, transitional basalts, trachybasalts, tepherites, melanonephelinites, nephelinites, trachyphonolites and carbornatites, while the silicic group includes phonolites, trachytes, rhyolites and associated pyroclastics (Baker et al., 1971; Macdonald, 1994, 2002; Macdonald et al., 1994). The volcanism was confined to the axial part of the rift in the Quaternary as mentioned above and is characterized by central volcanoes on the floor of the rift valley. These central volcanoes are associated with geothermal areas and 14 sites with potential for geothermal power development have been identified (Figure 2). Three of these sites (Olkaria, Eburru and Menengai) are at various stages of development. Olkaria and Eburru are currently producing and Menengai is in the exploration drilling stage.

FIGURE 2: Geothermal locations associated with the Kenyan section of the East African Rift Valley

2.2 Olkaria volcanic complex

The Greater Olkaria volcanic complex (GOVC) is a multicentre volcanic field covering an area of 240 km^2 (Figure 3). Olkaria does not have a single eruptive centre, unlike other axial volcanism centres on the floor of the rift that are characterized by a main eruption centre with summit craters or a caldera. Instead, the GOVC is a multicentre eruption field with at least 80 eruption centres, made of small steep

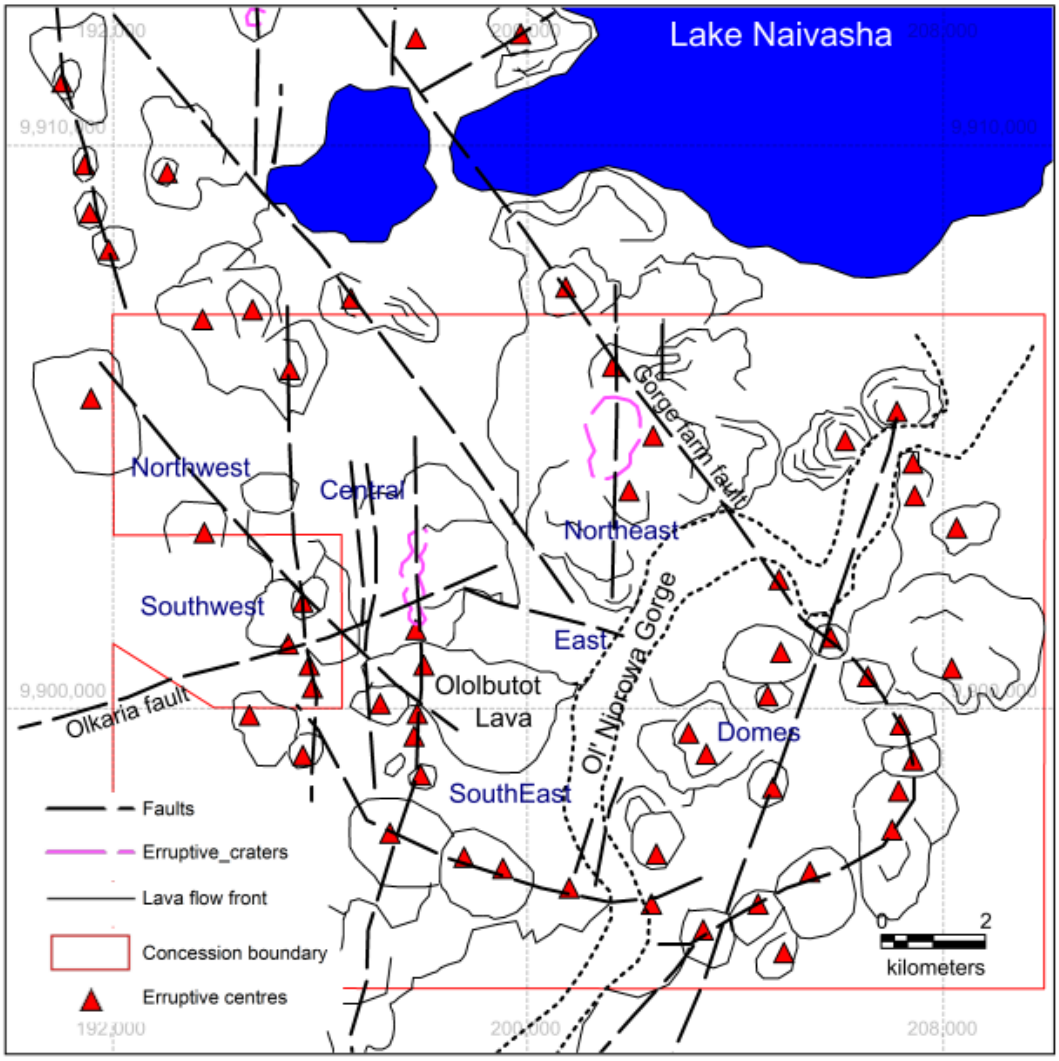

FIGURE 3: The Greater Olkaria geothermal area (modified from Karingithi et al. 2010)

sided domes composed of lava flows and or pyroclastics and thick lava flows of restricted extent. A group of arcuate aligned domes and associated lava flows in the south and south east of the field have been interpreted as surface expressions of a buried caldera (Naylor, 1972; Clarke et al., 1990).

The lava flows and the pyroclastic/lava domes are composed of peralkaline rhyolite (comendite). Olkaria and Eburru, are the only eruption centres where rhyolitic lava has erupted on the floor of the rift valley in Kenya. The genesis of the rhyolite volcanic suit has been discussed in detail (e.g., Davies and Macdonald, 1987; Macdonald et al., 1987) and may be attributed to partial melting of the crust aided by volatile flux or through protracted fractional crystallization of a mafic parent(s). The volcanic activity of the area surrounding Olkaria spans from 22-20,000 BP to 180±50y BP (e.g., MacDonald et al., 2008). Based on studies on rock cuttings from boreholes, the subsurface geology at Olkaria shows interchanging layers of rhyolite, trachyte, basalt and their associated pyroclastic and tuffs. Intrusions of rhyolite, basalt, syenite and granite in the form of dykes have been encountered in some wells in the field (e.g., Mwangi, 2012; Njathi, 2012; Okoo, 2013; Musonye, 2015; Otieno, 2016).

2.3 Olkaria geothermal development

The Olkaria geothermal area is a high-temperature volcanic hosted geothermal system associated with the greater Olkaria volcanic complex. The location of Olkaria is about 120 km northwest of Nairobi. Exploration for geothermal resources in the area started in the 1960s (Noble and Ojiambo, 1975). The progress was slow and steady but there was accelerated development from the year 2000 onwards. Today (as of December 2017) the installed geothermal capacity is 674 MW_e (Table 1).

TABLE 1: Installed capacity in Olkaria geothermal field

Year	Area	Power plant	Capacity [MW_e]	Operator
1981-1985	Olkaria East	Olkaria I	45	KenGen
2004	Olkaria central	Direct use and small scale electrical generation	4	Oserian
2014-2015	Olkaria East	Olkaria I AU 4 &5	150	KenGen
2003-2010	Olkaria Northeast	Olkari II	105	KenGen
2000-2014	Olkaria West	Olkaria III	140	Orpower 4 Inc.
2013	Olkaria Domes	Olkaria IV	150	KenGen
2011-2017		Wellheads	80	KenGen

Olkaria geothermal field is divided into seven sectors for development. These are Olkaria East (Olkaria I), Olkaria Northeast (Olkaria II), Olkaria West (Olkaria III), Olkaria Domes (Olkaria IV), Olkaria Southwest, Olkaria Northwest, and Olkaria central (Figure 3). The first power plant constructed in Olkaria was Olkaria I in the 1980s with a capacity of 45 MW_e. Following rising power demand after the year 2000, Olkaria II was built with a production capacity of 105 MW_e and Olkaria III with 139 MW_e. Additional development in the east field was carried out and a further 150 MW_e was added to the previous 45 MW_e. The Olkaria Domes was also developed at the same time and Olkaria IV with a 150 MW_e production capacity was installed in this sector (Figure 3). Kenya Electricity Generating Company (KenGen) operates Olkaria I, Olkaria I AU IV & V, Olkaria II and Olkaria IV power plants whereas Olkaria III is operated by OrPower 4 Inc. In addition, KenGen operates small wellhead generator units with a total production capacity of 81 MW_e and Oserian Development Company runs a 4 MW_e unit. Oserian also uses geothermal energy directly to heat greenhouses (Axelsson et al., 2017). Over 300 wells have been drilled in the KenGen concession area with depths ranging from 500 to 3500 m. Average production casing depth for the wells is 800 m.

2.4 Olkaria geothermal system

Olkaria geothermal system is a volcanic hosted high-temperature geothermal system. The heat source is believed to be magmatic, intruded into high levels in the crust (Macdonald and Scaillet, 2006). Micro-seismic studies done in Olkaria (Simiyu, 2000) revealed the presence of S-wave attenuating bodies at depths of 6-8 km below the surface and these are interpreted to represent bodies of partially molten material. The largest of these bodies are found in the Olkaria Domes, Olkaria North East and Olkaria West fields. Formation temperature distribution in the field coincides with these bodies and reflects hot upflow in the field and this is also supported by geochemical and geophysical data (Axelsson et al., 2017, 2013). The permeability in Olkaria is structurally controlled. Important structures in the field are oriented in the SW-NE (e.g., Olkaria fault), NW-SE and N-S directions (e.g., Gorge farm fault and Ololbutot fault, respectively). A structural and hydrological barrier divides Olkaria west and Olkaria east. This is represented by the N-S Ololbutot fault (Figure 3), and may represent a major down throw to the east. This hypothesis is supported by geology. In the west, the geothermal system is hosted in the Mau tuffs rocks, which are stratigraphically older than the trachyte hosting the reservoir to the east of the fault (Okoo, 2013; Owens et al., 2015). A basaltic cap rock is observed in the east field at depths of around 500 m below the surface, where there is a steam zone, which is a few hundred metres thick. A two-phase system exists below this steam cap. In other sectors, the fluid is two-phase and is liquid phase at deeper levels penetrated by the wells. The maximum bottom-hole temperature measured is 365ºC. Enthalpies in the field range from 950 to 2650 kJ/kg (Karingithi et al., 2010). At least four up flow zones have been identified in the field and they correspond with the high temperature areas associated with the heat sources seen in the field. The up flow zones are also collaborated by chemistry data and Na/K geothermometer temperatures. Chloride concentration increases in up flow zone areas although in some sectors the concentration may reflect the source and not progressive water rock interaction at elevated temperatures, for example in the southeast field.

It has been suggested that the recharge water into the geothermal system is a mixing series between meteoric water, from the flanks of the rift valley, and a deep axial flow source (Allen and Darling, 1987; Allen et al., 1989; Clarke et al., 1990; Nkapiani, 2014; Owens et al., 2015). This deep axial flow has also been interpreted as recharge from Lake Naivasha or water that has flowed for great lengths along the rifts due to the N-S structures on the rift floor that restrict flow across the rift. Shallow meteoric recharge also contributes to the recharge into the system in addition to the deep axial flow. Recharge in the Northeast and east field occurs via the Ololbutot fault and is seen in a temperature depression along the fault. A temperature depression also occurs between the Northeast and the East fields and has also been interpreted as a down flow in an earlier conceptual model by Ofwona, (2002). The Olkaria fault controls the upflow in the northeast and west field to a large extent. In the Domes, the ring structure forms a hydrological barrier and the geothermal resource in this area is confined to the west of this structure. Recharge into the Domes sector may be occurring along the ring structure, the Gorge farm fault and faults in the East of the sector along the Ol' Njorowa gorge.

2.5 Alteration mineralogy

The alteration mineralogy of the Olkaria geothermal system displays a typical pattern of high-temperature geothermal systems (Lagat, 2004; Mwangi, 2012; Njathi, 2012; Okoo, 2013; Musonye, 2015; Otieno, 2016). Alteration mineral zones are observed in order of increasing temperatures. A top zone (~0-200 m) is characterized by insignificant rock alteration (<40℃) followed by a smectite-zeolite zone (40-200°C), illite-chlorite zone (200-250°C), illite-chlorite-epidote zone (>250°C) and an epidote-actinolite-garnet-biotite zone (>280°C). In these zones, the first appearances of particular alteration mineral marks the hydrothermal alteration temperatures. The first appearance of epidote marks alteration temperatures of 250° C and above with actinolite indicating temperatures above 280° C. Garnet is rare in Olkaria wells and has only been observed through electron microprobe analysis. It indicates temperatures in excess of 300°C. Apart from the above mentioned mineral assemblages, other alteration minerals observed in Olkaria well cuttings include: fluorite, calcite, quartz, pyrite, chalcedony, scolecite, mesolite, phillipsite, laumontite, hematite, albite, chalcopyrite, sphene, wairakite, prehnite and wollastonite.

2.6 Fluid chemistry

The chemistry of the reservoir fluid in Olkaria geothermal field is dilute. The chloride content ranges from 40 to 940 ppm in the reservoir fluid, and it varies from one sector to another, as well as between parts of the same sector, which may reflect the extent of water-rock interaction or the source of supply. The reservoir temperatures calculated from Na/K geothermometer range from 240 to 300°C and the reservoir pH ranges from 6.5 to 7.0. Fluoride concentration is high with an average of 45 ppm compared to other volcanic hosted systems (generally < 10 ppm) for example in Iceland (Arnórsson et al., 2007). The high fluoride concentration may be attributed to the high content of halogens in obsidians (F >1% and Cl > 0.5% max.) found in the volcanic assemblage in Olkaria (Macdonald et al., 1987). Carbon dioxide (CO_2) concentrations in the fluids are highest in Olkaria West or up to 22,000 ppm in the reservoir. In the other sectors, the average CO_2 concentration in the reservoir fluid is 700 ppm. In some sectors in Olkaria (e.g. E and NE) the concentration of CO_2 in the reservoir fluid is controlled by close approach to equilibrium with a prehnite-clinozoisite-calcite-quartz mineral assemblage while in others (West and parts of the Domes) it is fixed externally by a flux from a magmatic source to the convecting fluid (Karingithi, 2002; Karingithi et al., 2010). H_2S content in the reservoir fluid is variable (3.5-62.6 ppm) and is highest in the East field (up 62.6 ppm) and lowest in the West sector. The concentration of H_2 in the reservoir fluid ranges from 0.01-1.66 ppm. It also follows the same distribution pattern in the reservoir as H_2S, that is, lowest in the West sector and highest in the East sector. The concentration of H_2S and H_2 is controlled by close approach to equilibria between solution and specific mineral assemblage, either pyrite-pyrrhotite-magnetite or pyrite-pyrrhotite-prehnite-epidote (Karingithi et al., 2010). The initial aquifer waters (prior to boiling) show a close approach to equilibria with Ca bearing minerals but this equilibria may locally be upset by boiling induced by depressurization around wells and also the high CO_2 influx from the magma heat source.

3. SAMPLING AND ANALYSIS

3.1 Sampling

A total of 17 two-phase well discharge samples were collected in November 2017. Wells from various sectors were chosen for the sampling. The selection was based on geology, fluid chemistry and discharge enthalpy or vapour to liquid ratio. Sample locations are shown in Figure 4.

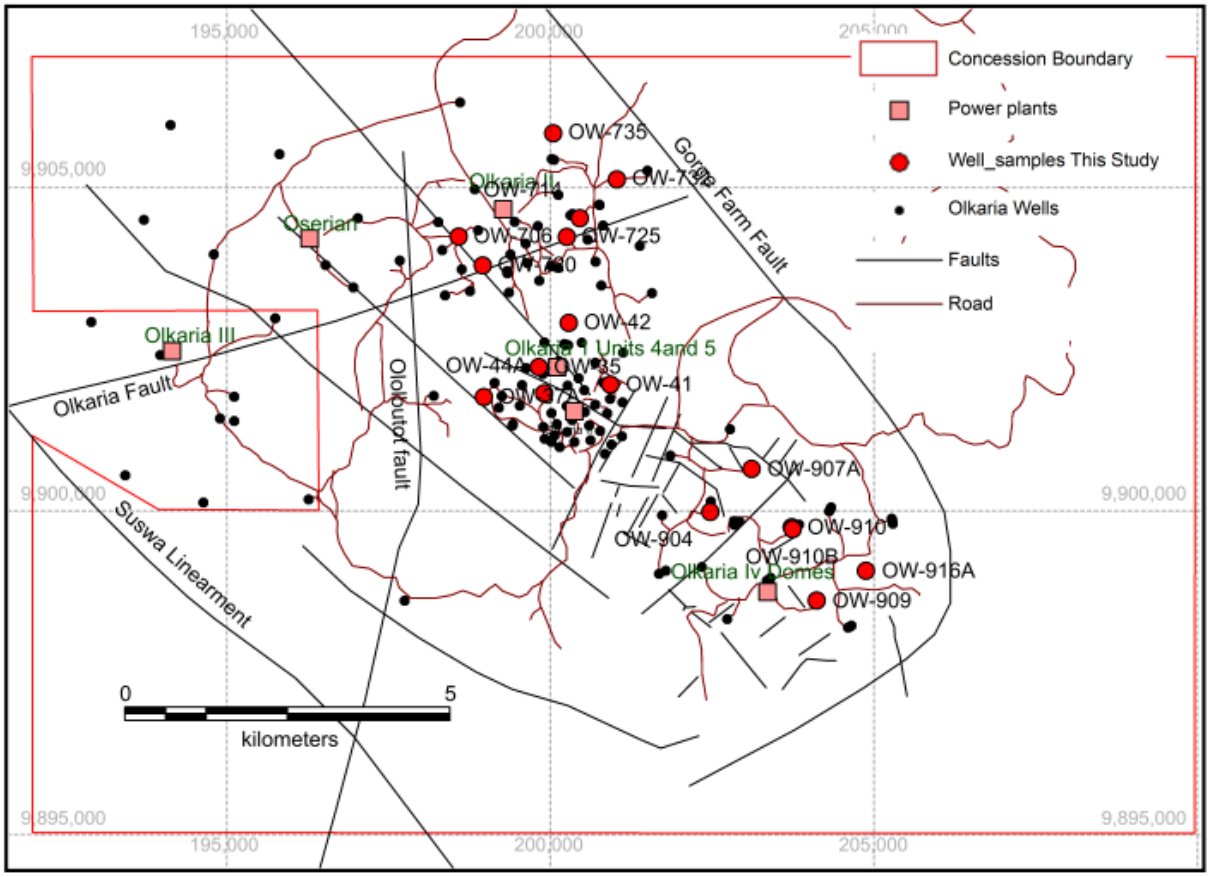

FIGURE 4: Well locations in Olkaria geothermal field; the red dots represent wells chosen for this study. Important structures in the field are also shown

All samples collected were of two-phase well discharges, and were collected at the wellhead. The vapour and liquid phases were separated using a Webre separator. Prior to sampling the Webre separator was flashed for around 5 minutes. It should be noted that liquid samples were not collected at the weir box as commonly done; such sample locations may be effected by evaporation.

Samples for major volatiles (H_2O, H_2S, CO_2, H_2, N_2, Ar, CH_4) analysis in the vapour phase were collected into pre-evacuated gas bulbs containing 50% KOH (w/w), around10 mL per 100 mL of gas bulb volume. Separate samples were collected for isotope analysis (δD and $\delta^{18}O$) of the H_2O of the vapour phase. For these samples, the vapour phase was condensed in-line using a stainless steel cooling coil and the vapour condensate collected into high-density polyethylene (HDPE) bottles.

Samples of major elements (pH, Si, B, Na, K, Ca, Mg, Fe, Al, Cl, F, CO_2, H_2S) in the liquid phase were also collected directly from the Webre separator. The samples were cooled using an in-line stainless steel cooling coil. Samples for determination of pH, total dissolved inorganic carbon (CO_2) and total dissolved sulphide (H_2S) were collected into glass flasks. For other major elements, the samples were filtered through a 0.2µm filter (cellulose acetate) using a Nalgene vacuum filter holder into HDPE plastic bottles. For cation determination, the samples were further acidified to 1% HNO_3 (Merck Suprapur). For SO_4 analysis, 1 ml of a 2% Zn-acetate solution was added to preserve the samples. For F and Cl

determination, the samples were not further treated. Separate samples were collected for isotope analysis (δD and $\delta^{18}O$) of the H_2O of the liquid phase. For these samples, the liquid phase was cooled in-line using a stainless steel cooling coil and collected into HDPE bottles.

3.2 Chemical analysis

For the liquid phase, dissolved H_2S was analysed on site by Hg-precipitation titration using dithizone as an indicator (Arnórsson et al., 2006). pH and CO_2 was analysed within a few days using a combination electrode and modified alkalinity titration (Stefánsson et al., 2007). The concentrations of major cations (SiO_2, B, Na, K, Ca, Mg, Al, and Fe) were determined using inductively coupled optical emission spectroscopy (ICP-OES). Major anions (F, Cl and SO_4) were analysed using ion chromatography (IC, Dionex 2000).

For the vapour phase, the condensable gases, CO_2 and H_2S, were analysed using modified alkalinity titration (Stefánsson et al., 2007) and Hg-acetate precipitation titration with dithizone as an indicator, respectively (Arnórsson et al., 2006). The non-condensable gases (H_2, CH_4, N_2 and Ar) were analysed using gas chromatography (GC) and the H_2O determined by gravimetry and mass balance.

The analytical precision for all major elements based on duplication determination was found to be <3% at the 95% confidence level and for pH <±0.05.

3.3 Isotope analysis

The analysis of isotopes was carried out using a Thermo Delta V advantage Isotope Ratio Mass Spectrometer (IR-MS). Prior to analysis, 1% Zn-acetate solution was added to the samples to remove any dissolved sulphide that may potentially interfere with the measurements. The precipitate formed was subsequently filtered off using 0.2 µm filter (cellulose actetate). The samples were put in vials (200µl sample in 12ml vials) where they were flushed with a gas. The flush gas used for oxygen isotope measurements consisted of 99.7% He and 0.3% CO_2. After flushing, the samples were reacted for over 24 hours prior to analysis. The flush gas used for hydrogen isotope measurements consisted of 98% He and 2% H_2. The reaction time after flushing was over 1 hour. For hydrogen measurements, a titanium stick was inserted in each vial and served as a catalyst and thus speeded up the reaction between the flush gas and the sample. The reaction temperature was set at 22±0.5°C. Following the reaction time the gas mixture is cleaned in-line using water traps and a GC column followed by analysis using the mass spectrometer. Each sample was measured ten times and the average of eight used to calculate the respective isotope value.

The hydrogen and oxygen isotope ratios are reported relative to an international reference material, using the standard notation:

$$\delta D = \left(\frac{\left({}^{2}H/{}^{1}H \right)^{sample}}{\left({}^{2}H/{}^{1}H \right)^{standard}} - 1 \right) \times 1000 \quad (1)$$

$$\delta^{18}O = \left(\frac{\left({}^{18}O/{}^{16}O \right)^{sample}}{\left({}^{18}O/{}^{16}O \right)^{standard}} - 1 \right) \times 1000 \quad (2)$$

The standard used as a reference for reporting hydrogen and oxygen isotopes, is the Vienna Standard Mean Ocean water (V-SMOW) and the ratios are given in per mill (‰). The final values were corrected for the addition of zn-acetate added to the samples prior to analysis.

The analytical precision obtained by repeated analysis is <1.0‰ for δD and <0.1‰ for $\delta^{18}O$.

4. GEOCHEMICAL AND ISOTOPE MODELLING

4.1 Model setup

The vapour and liquid samples collected at surface from well discharges have undergone chemical and isotope changes upon ascent from the reservoir to the surface. Assuming the system to be thermodynamically closed, these changes involve adiabatic boiling from the reservoir to the point of sampling. In addition, the reservoir may be assumed to consist of a single liquid phase or a two-phase system of vapour and liquid. In order to study the effects of boiling, two model scenarios were made: (1) single phase liquid reservoir followed by adiabatic boiling to surface and (2) progressive vapour formation upon isobaric boiling. In the former case, the total enthalpy (h) of the system is kept constant and the pressure and temperature of the system decreased along the two-phase curve, whereas in the latter case, the enthalpy is allowed to increase at constant pressure and temperature. The two model setups are demonstrated in Figure 5.

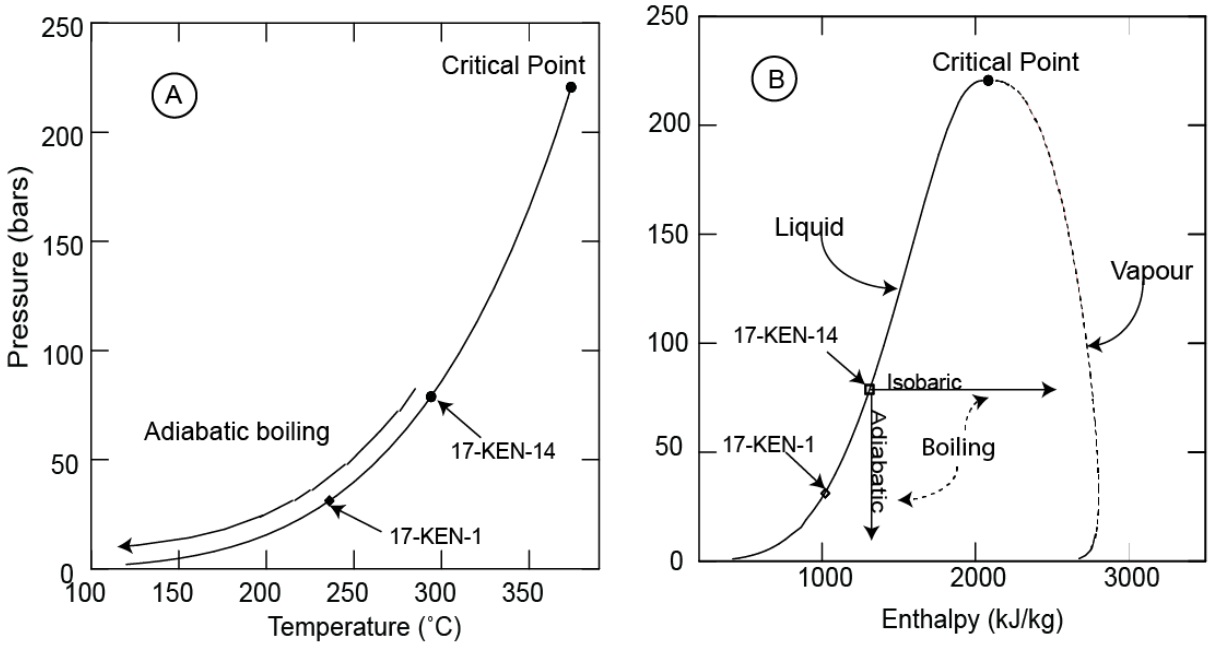

FIGURE 5: The model setup used to study the effects of boiling on isotope composition. Adiabatic boiling assumes constant enthalpy and decreasing temperature and pressure along the water vapour curve, whereas isobaric boiling assumes increasing enthalpy, by heat addition at constant temperature and pressure

In both cases the vapour fraction is related to the total enthalpy of the system, and the enthalpy of liquid water and vapour through:

$$h^{total} = x^v h^v_{T,P} + x^{lq} h^{lq}_{T,P} = x^v h^v_{T,P} + (1 - x^v) h^{lq}_{T,P} \quad (3)$$

where h^{total} is the total enthalpy of the system, $h^v_{T,P}$ is the enthalpy of vapour at a given temperature and pressure, $h^{lq}_{T,P}$ is the enthalpy of liquid water at a given temperature and pressure, and x^v and x^{lq} are the vapour and liquid fractions, respectively.

By solving Equation 3, the vapour fraction can be calculated by:

$$x^v = \frac{h^{total} - h^{lq}_{T,P}}{h^v_{T,P} - h^{lq}_{T,P}} \quad (4)$$

4.2 Calculation of the effects of boiling and reservoir fluid composition

For a closed thermodynamic system, mass is conserved. It follows that the total mass of a component i is given by:

$$m_i^{total} = x^v m_i^v + (1 - x^v) m_i^{lq} \quad (5)$$

For non-volatile elements (e.g. Cl) only present in the liquid phase, $m_i^v = 0$ and for volatile elements (e.g. H_2) only present in the vapour phase, $m_i^{lq} = 0$. For elements present in both phases like H_2O, H_2S and CO_2, the ratio between the two needs to be determined.

In order to calculate the reservoir fluid chemical composition using the above formulas and from data on vapour and liquid water composition at surface, one needs to determine the enthalpy and the temperature of the system or reservoir. Here, the reservoir temperatures were calculated using quartz geothermometry (Fournier and Potter, 1982). The enthalpy was obtained in two ways: (1) assuming liquid only reservoir, i.e. $h^{total} = h^{lq}_{T^{res}, P^{res}}$ where T^{res} and P^{res} are the reservoir temperatures and pressures, respectively; (2) using the measured fluid discharge enthalpy. The calculations were carried out with the aid of the WATCH program version 2.4 (Arnórsson et al., 1982; 1983; Bjarnason, 2010).

4.3 Calculation of the effects of boiling on δD and $\delta^{18}O$ and the reservoir δD and $\delta^{18}O$ values

The hydrogen and oxygen isotope systematics of H_2O were further constrained as a function of the two boiling model setups.

The total δD and $\delta^{18}O$ isotope values of H2O of the system is defined according to:

$$\delta D^{system} = x^v \delta D^v + x^{lq} \delta D^{lq} \quad (6)$$

$$\delta^{18} O^{system} = x^v \delta^{18} O^v + x^{lq} \delta^{18} O^{lq} \quad (7)$$

where x^v and x^{lq} are the vapour and liquid H_2O fractions, respectively.

The vapour-liquid H_2O isotope reactions of δD and $\delta^{18}O$ can be described by:

$$HDO_{(v)} + H_2O_{(lq)} = H_2O_{(v)} + HDO_{(lq)} \quad (8)$$

$$H_2{}^{18}O_{(v)} + H_2O_{(lq)} = H_2O_{(v)} + H_2{}^{18}O_{(lq)} \quad (9)$$

and the respective fractionation factors are defined by:

$$\alpha_{lq-v}(D) = \frac{1000 + \delta D^{lq}}{1000 + \delta D^v} \quad (10)$$

$$\alpha_{lq-v}\left({}^{18}O\right) = \frac{1000 + \delta^{18} O^{lq}}{1000 + \delta^{18} O^v} \quad (11)$$

where (Horita and Wesolowski, 1994):

$$10^3 ln\alpha_{lq-v}(D) = 1158.8\frac{T^3}{10^9} - 1620.1\frac{T^2}{10^6} + 794.84\frac{T}{10^3} - 1620.1 + 2.9992\frac{10^9}{T^3} \quad (12)$$

$$10^3 ln\alpha_{lq-v}\left({}^{18}O\right) = -7.685 + 6.7123\frac{10^3}{T} - 1.6664\frac{10^6}{T^2} + 0.35041\frac{10^9}{T^3} \quad (13)$$

T is temperature in K.

Solving the equations together results in the calculations of δD and $\delta^{18}O$ isotope values of H_2O as a function of steam fraction and temperature:

$$\delta D^{system} = x^v \delta D^v + (1 - x^v)\left(\alpha_{lq-v}(D)(1000 + \delta D^v) - 1000\right) \quad (14)$$

$$\delta^{18}O^{system} = x^v \delta^{18}O^v + (1 - x^v)\left(\alpha_{lq-v}\left({}^{18}O\right)(1000 + \delta^{18}O^v) - 1000\right) \quad (15)$$

$$\delta D^{system} = x^v\left(1/\alpha_{lq-v}(D)\left(1000 + \delta D^{lq}\right) - 1000\right) + (1 - x^v)\delta D^{lq} \quad (16)$$

$$\delta^{18}O^{system} = x^v\left(1/\alpha_{lq-v}\left({}^{18}O\right)\left(1000 + \delta^{18}O^{lq}\right) - 1000\right) + (1 - x^v)\delta^{18}O^{lq} \quad (17)$$

$$\delta D^v = \frac{\delta D^{system} + 1000\left(-\alpha_{lq-v}(D) + 1 + x^v\alpha_{lq-v}(D) - x^v\right)}{x^v - \alpha_{lq-v}(D) + x^v\alpha_{lq-v}(D)} \quad (18)$$

$$\delta^{18}O^v = \frac{\delta^{18}O^{system} + 1000\left(-\alpha_{lq-v}\left({}^{18}O\right) + 1 + x^v\alpha_{lq-v}\left({}^{18}O\right) - x^v\right)}{x^v - \alpha_{lq-v}\left({}^{18}O\right) + x^v\alpha_{lq-v}\left({}^{18}O\right)} \quad (19)$$

$$\delta D^{lq} = \frac{\delta D^{system} + 1000\left(-x^v\, 1/\alpha_{lq-v}(D) + x^v\right)}{x^v\, 1/\alpha_{lq-v}(D) + 1 - x^v} \quad (20)$$

$$\delta^{18}O^{lq} = \frac{\delta^{18}O^{system} + 1000\left(-x^v\, 1/\alpha_{lq-v}\left({}^{18}O\right) + x^v\right)}{x^v\, 1/\alpha_{lq-v}\left({}^{18}O\right) + 1 - x^v} \quad (21)$$

The isotope calculations were carried out using the IsoGem program (Stefánsson et al., in prep.).

5. RESULTS

5.1 Chemical composition

The chemical composition of liquid water and vapour from Olkaria at sampling conditions is given in Table 2 and the relative abundance of components are shown in Figure 6. Both the liquid and vapour phases are dominated by H_2O with mol% of 99.8-99.9 and 98.9-99.8, respectively. Following water, Na, SiO_2 and Cl are the most important components in the liquid phase with concentrations of 153-1017, 465-890 and 119-1267 ppm, respectively. K, F, CO_2, SO_4, H_2S also displayed elevated concentrations whereas Ca, Mg, Al and Fe generally had concentrations on the lower ppm and ppb level. In the vapour phase, CO_2 and H_2 were the dominant components after water with concentrations of 67.8-586 mmol/kg and 8.75-56.5 mmol/kg, respectively, followed by H_2S, N_2, CH_4 and Ar.

5.2 Isotope composition

The results of the δD and $\delta^{18}O$ isotope analysis in liquid and vapour phases are presented in Table 3. The δD and $\delta^{18}O$ isotopes of the liquid phase ranged from -3.2 to +9.0‰ and -1.45 to +1.31‰, respectively. The δD and $\delta^{18}O$ isotope of the vapour phase ranged from +0.8 to +16.1‰ and +0.78 to +3.18‰, respectively. The spread of the isotope values for δD and $\delta^{18}O$ measured is shown in Figure 7.

In addition to the data set obtained, data set from previous work (Allen and Darling, 1987; Sveinbjörnsdóttir, 1988; Allen et al., 1989; Ojiambo and Lyons, 1993; Karingithi, 2000; Ojiambo et al., 2001) and KenGen internal data from analyses carried out in 2014. 42% of the data set from previous reports is composed of liquid-phase only samples, taken at the weirbox (at atmospheric pressure). The other samples are composed of two-phase samples (liquid and vapour), the liquid phase collected at atmospheric conditions and the vapour phase sampled at higher pressure. The data set obtained in 2014 is composed of liquid- and vapour-phase samples collected at the same pressure. The δD and $\delta^{18}O$ isotope values of the liquid phase for the older data set ranges from -9.3 to +32.9‰ and -4.55 to +6.36‰, respectively, while the δD and $\delta^{18}O$ values of the vapour phase range from -4.2 to +10.86 ‰ and -2.50 to +1.16‰, respectively. Figure 8 gives a distribution of this dataset.

TABLE 2: Chemical component concentration of two-phase Olkaria geothermal fluid

Sample #	Well #	Ps	h	Liquid phase (ppm)													Vapour phase (mmol/kg)						
		[bar-g]	[kJ/kg]	pH	@°C	SiO_2	B	Na	K	Ca	Mg	Al	Fe	F	Cl	CO_2	SO_4	H_2S	CO_2	H_2S	H_2	N_2	Ar	CH_4
17-KEN-1	OW-41[b]	10.9	2747	8.34	25	465		190	47.7	0.503	0.030	2.07	0.051	73.3	119	65.0	4.70	7.31	144	4.42	22.4	0.71	0.016	0.094
17-KEN-2	OW-725[c]	5.5	2180	9.49	25	472	2.52	468	57.1	0.685	0.026	1.45	0.026	43.1	301	193		38.2[a]	313	15.4	34.1	1.44	0.028	0.716
17-KEN-4	OW-37A[b]	11.5	2240	9.88	25	653	7.93	1017	283	0.297	0.014	0.602	0.017	168	1267	29.0	108	34.4	67.8	6.60	12.0	4.34	0.065	0.286
17-KEN-5	OW-44A[b]	10.7	2670	8.48	25	646		633	188	0.726	0.023	1.25	0.016	78.6	915	39.0	44.4	11.2	102	2.34	18.5	1.43	0.028	0.330
17-KEN-6	OW-907A[d]	11.0	1786	9.57	25	637	1.58	315	52.9	0.479	0.024	1.38	0.022	50.0	125	253	17.7	18.1	586	0.065	20.7	1.43	0.028	1.59
17-KEN-7	OW-910[d]	17.0	2049	9.85	25	689	3.08	403	83.0	0.216	0.008	0.819	0.025	128	240	111	9.18	18.9	159	3.06	25.5	0.91	0.020	0.462
17-KEN-8	OW-35[b]	14.0	2301	9.89	25	709	10.2	573	126	0.459	0.026	1.90	0.019	85.2	633	11.0	23.8	0.53[a]	447	0.129	56.5	1.43	0.028	0.652
17-KEN-9	OW-910B[d]	15.0	1756	10.07	25	625	1.74	388	70.1	0.442	0.023	1.39	0.027	55.9	134	242	15.1	56.2	244	3.88	19.8	1.51	0.033	0.793
17-KEN-12	OW-714[c]	5.7	1754	9.98	25	630	2.63	512	79.4	0.505	0.024	1.44	0.020	72.4	446	58.0	31.4	68.0	232	11.9	22.0	1.44	0.028	0.580
17-KEN-13	OW-916A[d]	11.0	2144	9.55	25	754	3.66	547	117	0.564	0.025	1.19	0.025	230	276	159	7.03	16.7	203	2.38	26.7	0.72	0.017	1.45
17-KEN-14	OW-732[c]	11.0	1725	9.50	25	890	3.48	425	105	0.757	0.031	1.66	0.052	52.7	481	62.5	6.08	26.7	224	8.60	37.7	2.23	0.052	1.04
17-KEN-15	OW-42[b]	11.5	2718	6.20	25	605		153	30.1	0.880	0.029	4.12	0.255	33.8	202	110	9.59	0.52	71.0	4.19	8.79	0.68	0.013	0.080
17-KEN-16	OW-720[c]	6.8	2287	10.14	25	483	2.18	436	50.7	0.594	0.023	1.02	0.025	61.5	260	20.4	64.0	24.6[a]	140	3.22	18.6	1.43	0.028	0.372
17-KEN-17	OW-904[d]	11.0	1568	10.06	25	574	1.52	451	72.3	0.554	0.030	1.21	0.027	52.5	123	322	13.0	2.15[a]	497	0.317	31.9	1.45	0.028	3.43

[a] Calculated based on H_2S in the steam phase and steam-liquid equilibria; [b] Olkaria East field; [c] Olkaria North East field [d] Olkaria Domes

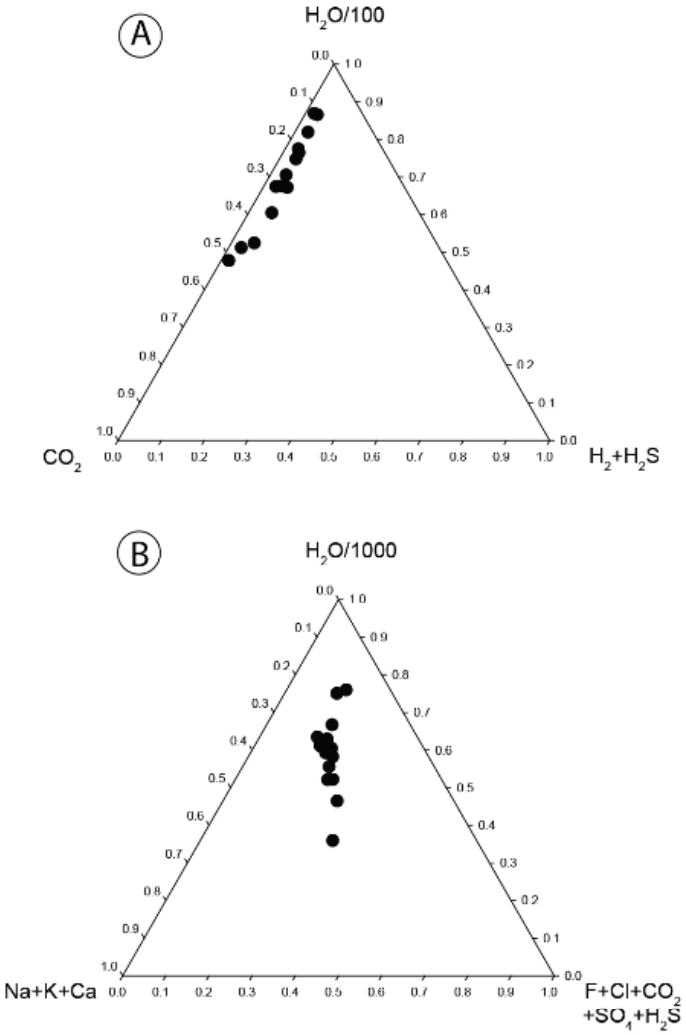

FIGURE 6: Ternary relationship between major components in the vapour; and B) liquid phases at Olkaria

TABLE 3: Isotope composition of liquid water and water steam of Olkaria geothermal field

Sample #	Well #	P^s [bar]	Liquid phase		Vapour phase	
			δD ‰	$\delta^{18}O$ ‰	δD ‰	$\delta^{18}O$ ‰
17-KEN-1	OW-41	10.9	5.9	2.76	6.2	1.31
17-KEN-2	OW-725	5.5	14.3	2.11	5+.3	-0.93
17-KEN-3	OW-735	8.3	9.5	1.65	2.1	-1.28
17-KEN-4	OW-37A	11.5	0.8	0.78	-3.7	-1.45
17-KEN-5	OW-44A	10.7	2.2	2.18	-0.2	-0.13
17-KEN-6	OW-907A	11	9.0	1.52	6.7	-0.58
17-KEN-7	OW-910	17	8.9	2.29	7.0	0.24
17-KEN-8	OW-35	14	2.9	1.34	-1.0	-0.05
17-KEN-9	OW-910B	15	6.4	1.73	4.6	-0.28
17-KEN-10	OW-909	11.5	10.1	2.70	4.7	0.21
17-KEN-12	OW-714	5.7	12.8	1.92	3.9	-0.65
17-KEN-13	OW-916A	11	16.1	3.18	9.0	0.57
17-KEN-14	OW-732	11.1	10.2	1.76	4.5	-0.47
17-KEN-15	OW-42	11.46	11.1	2.69	7.4	0.67
17-KEN-16	OW-720	6.78	12.7	1.39	4.9	-1.23
17-KEN-17	OW-904	11	12.9	2.12	6.2	-0.56

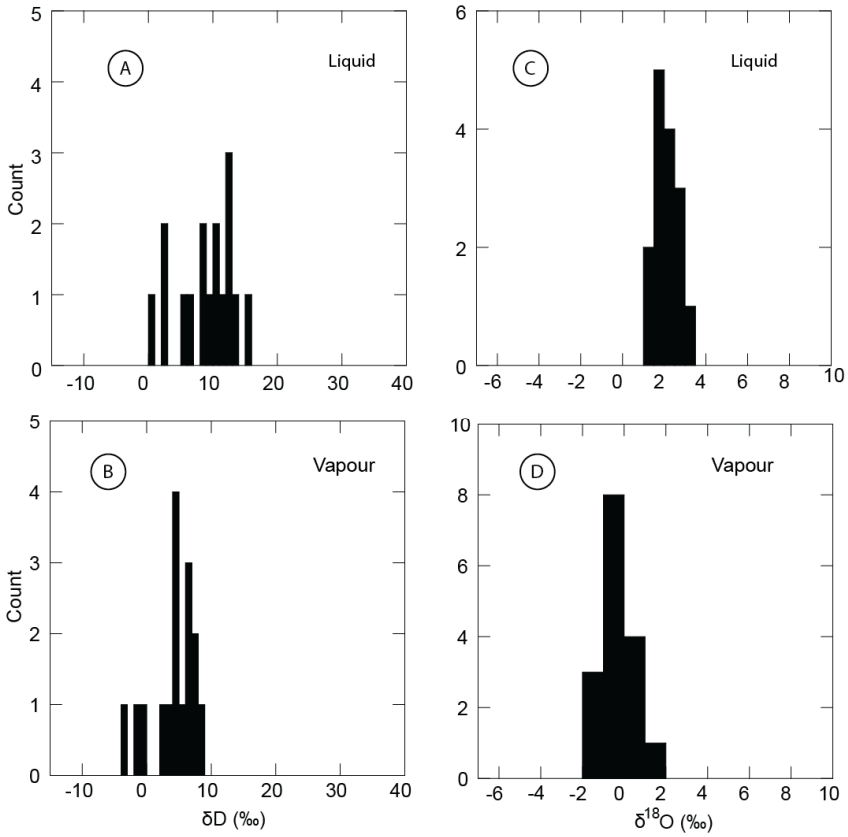

FIGURE 7: Distribution of δD and $\delta^{18}O$ in vapour and liquid phase of Olkaria geothermal fluid sampled in this study

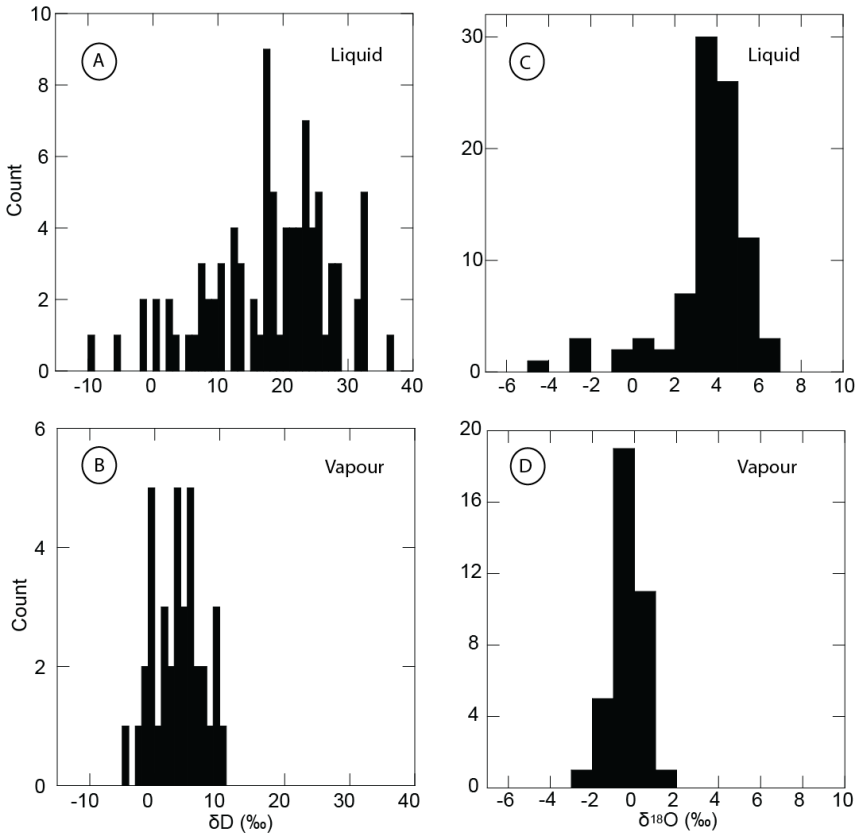

FIGURE 8: Distribution of δD and $\delta^{18}O$ in Olkaria vapour and liquid geothermal discharges reported in previous studies

6. DISCUSSION

6.1 Effects of boiling on fluid composition and δD and $\delta^{18}O$ systematics

In order to study the effects of adiabatic boiling and isobaric boiling on the δD and $\delta^{18}O$ compositions of the liquid and vapour phases, forward type modelling was conducted (see Section 4). For demonstration, two samples (17-KEN-1 (OW-41) and 17-KEN-14 (OW-732)) were selected. First, the chemical and isotope composition of the reservoir fluid was assessed. The reservoir composition was taken as the system values, i.e. m_i^{total}, δD^{system} and $\delta^{18}O^{system}$ (Equations 5-7). The selection of these samples was based on two different reservoir temperatures (237 and 294°C) but was otherwise entirely arbitrary.

Upon adiabatic boiling, the vapour fraction (x_i) progressively increases at constant enthalpy as the temperature and pressure of the system decreases (Figure 9). As a result, the concentrations of non-volatile components like Cl increase in the liquid phase due to removal of H_2O into the vapour phase (Figure 10). For volatile components, like H_2S and H_2, their concentrations increase rapidly in the vapour phase upon initial boiling followed by a concentration decrease due to dilution and addition of H_2O into the vapour phase upon increased vapour fraction (Figure 11).

The effects of boiling on δD and $\delta^{18}O$ are shown in Figure 9. Upon excessive boiling the liquid phase becomes enriched in D and ^{18}O, resulting in the δD and $\delta^{18}O$ values becoming higher and lower for the liquid and vapour phases, respectively. This is caused by fractionation of the heavy isotopes between the liquid phase and the vapour phase. According to experiments on fractionation of ^{18}O and D in water between the liquid phase and vapour phase upon boiling (e.g. Horita and Wesolowski, 1994), at all temperatures below the critical temperature of water (374°C), the liquid phase is enriched with ^{18}O. This results in an increase of $\delta^{18}O$ value in the liquid phase and a decrease of $\delta^{18}O$ values in the vapour phase upon progressive boiling to low temperatures. For D, the vapour phase is enriched upon boiling from the critical temperature up to 230°C, so that the δD values in the vapour phase increase and the δD values in the liquid phase decrease. At temperatures 220-230°C (cross over temperature) fractionation of D between the liquid phase and the vapour phase is indistinguishable. Below the cross over temperature, D is enriched in the liquid phase, so that δD values increase in the liquid phase and decrease in the vapour phase with progressive boiling below the cross over temperature to low temperatures. As observed in Figure 9, adiabatic boiling can result in substantial changes of the δD and $\delta^{18}O$ ratios from the reservoir conditions, considered to reflect the source, to the sampling conditions. In the case of Olkaria geothermal fluids, the fractionations for δD may be as high as 30‰ at reservoir temperatures up to 100°C (at the surface) and the fractionations for $\delta^{18}O$ may be has high as 5‰ at reservoir temperatures up to 100°C. Evaporation at 100°C may further increase the fractionation making the vapour phase progressively more depleted in D and ^{18}O and the liquid phase enriched in D and ^{18}O.

Isobaric boiling was observed to result in similar chemical and isotopic changes for the liquid and vapour phases as adiabatic boiling. As enthalpy increases in the system, for example by magmatic heat addition, the vapour fraction increases, eventually turning the system into vapour (Figure 11). As in the case of adiabatic boiling, the concentrations of non-volatiles like Cl increase in the liquid phase whereas the concentrations of volatiles like H_2S and H_2 initially increase in the vapour phase followed by decrease due to addition of vapour H_2O (Figure 12). In contrast, the δD and $\delta^{18}O$ systematics follow a different trend upon progressive isobaric boiling compared to adiabatic boiling. As the boiling occurs at constant temperature, the fractionation of δD and $\delta^{18}O$ between the vapour and liquid phase stays constant (α is constant). The absolute values, however, change with increasing vapour fraction with the δD and $\delta^{18}O$ of the vapour phase progressively approaching those of the system.

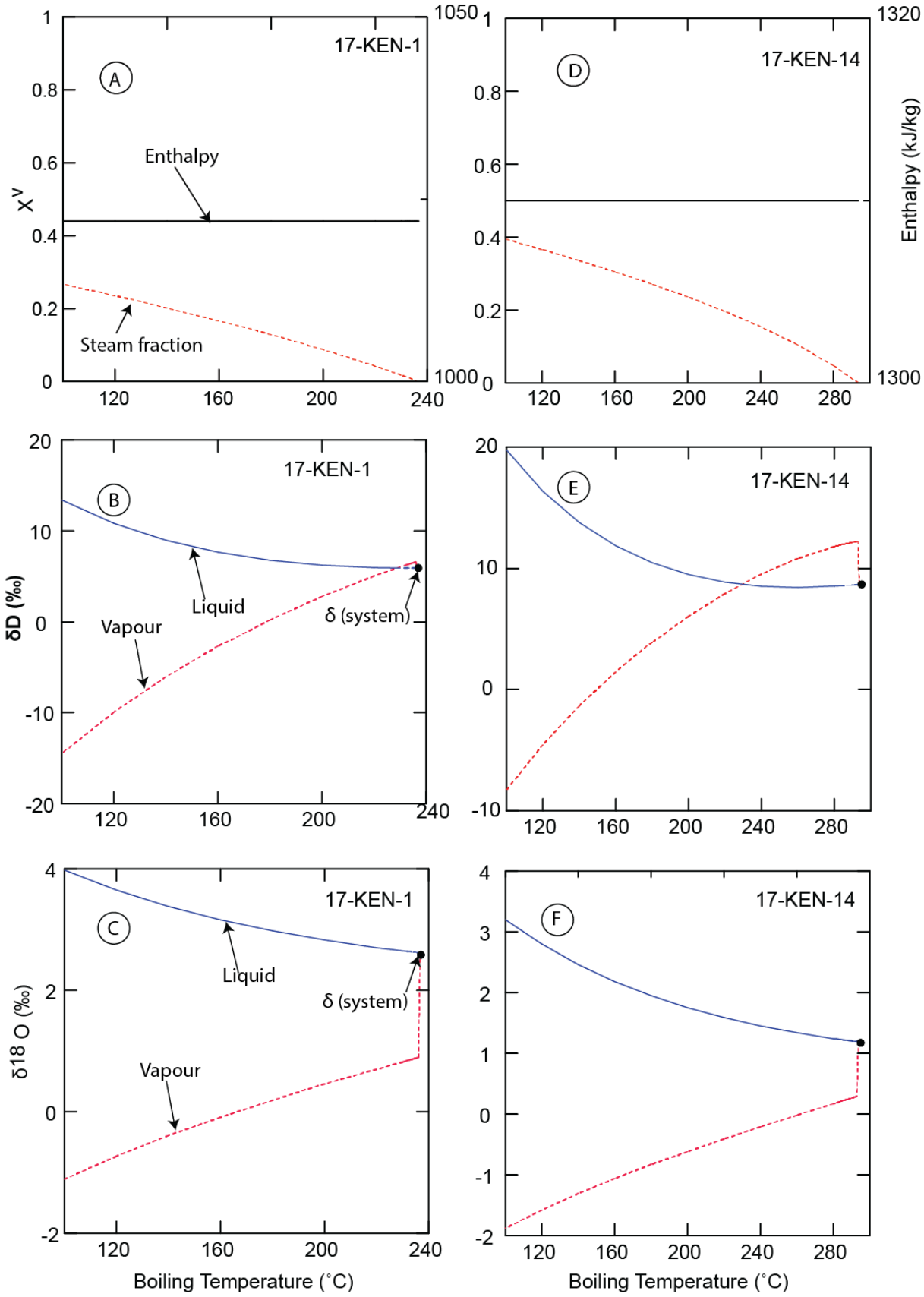

FIGURE 9: Steam fraction and isotope value evolution of reservoir fluid of 17-KEN-1 and 17-KEN-14 upon adiabatic boiling

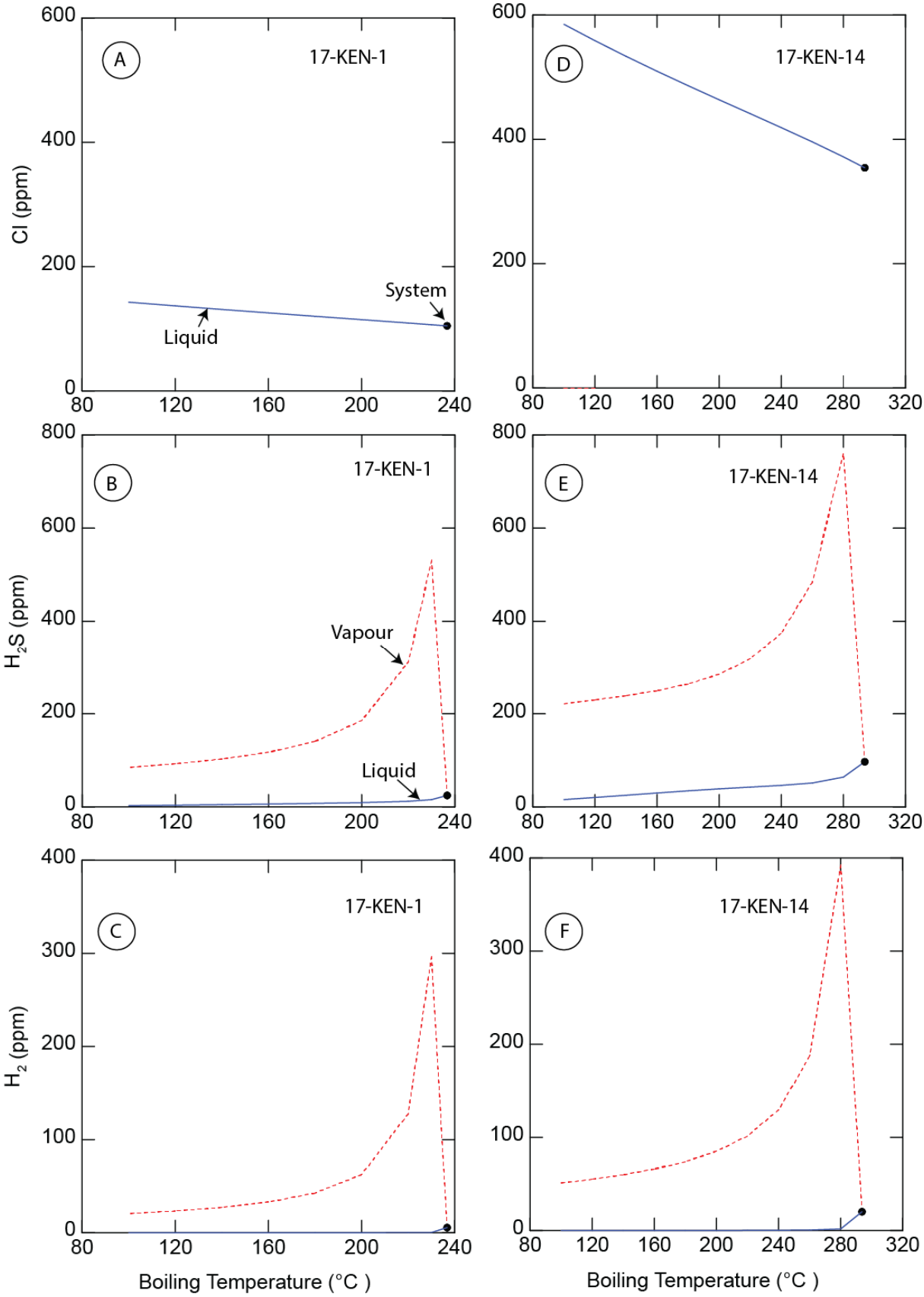

FIGURE 10: Example of major element and gas concentration changes (Cl, H_2S and H_2) in liquid and vapour phases upon adiabatic boiling of reservoir fluids

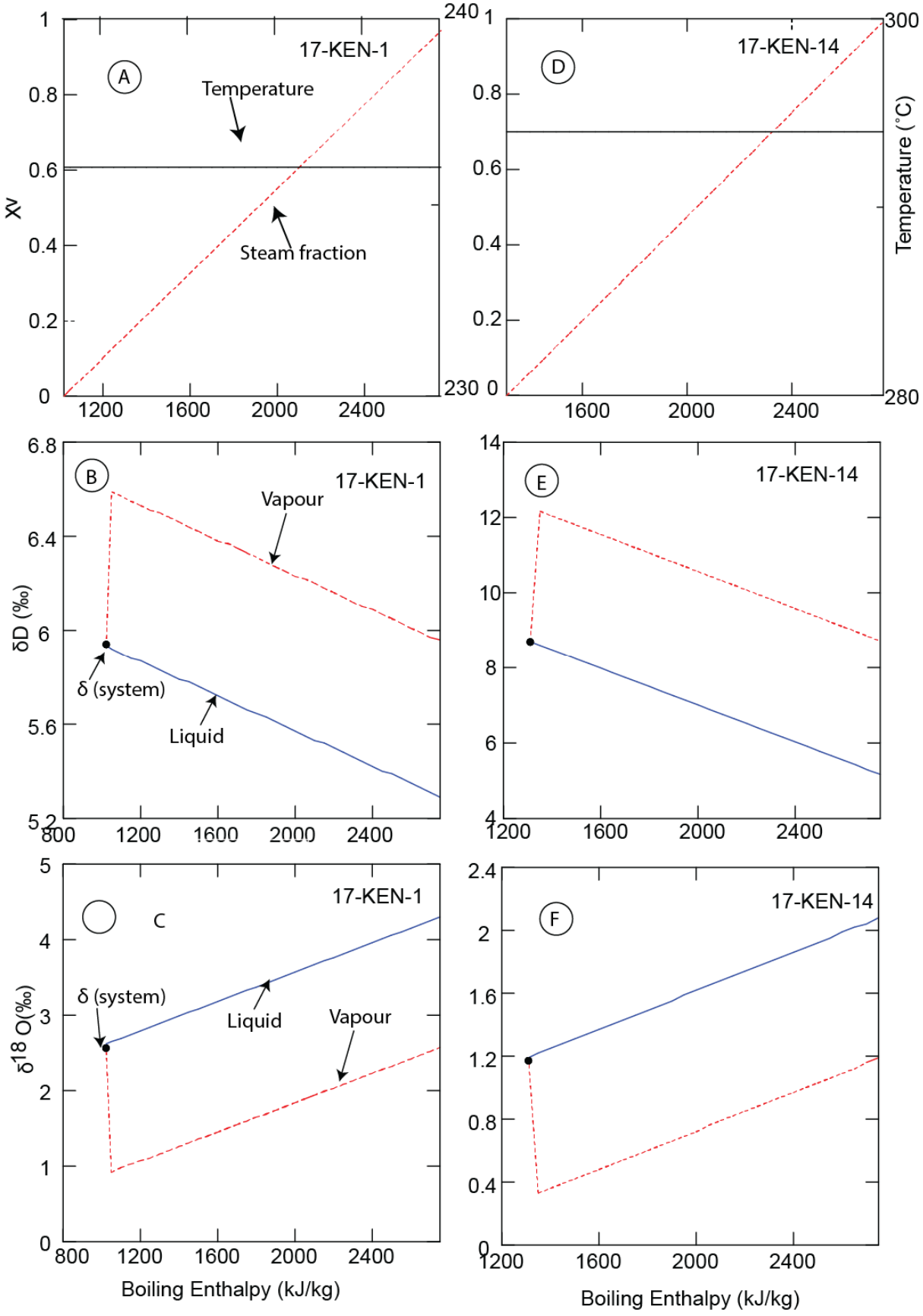

FIGURE 11: Vapour fraction and isotope value evolution of reservoir fluid of 17-KEN-1 and 17-KEN-14 upon isobaric boiling of the reservoir fluid

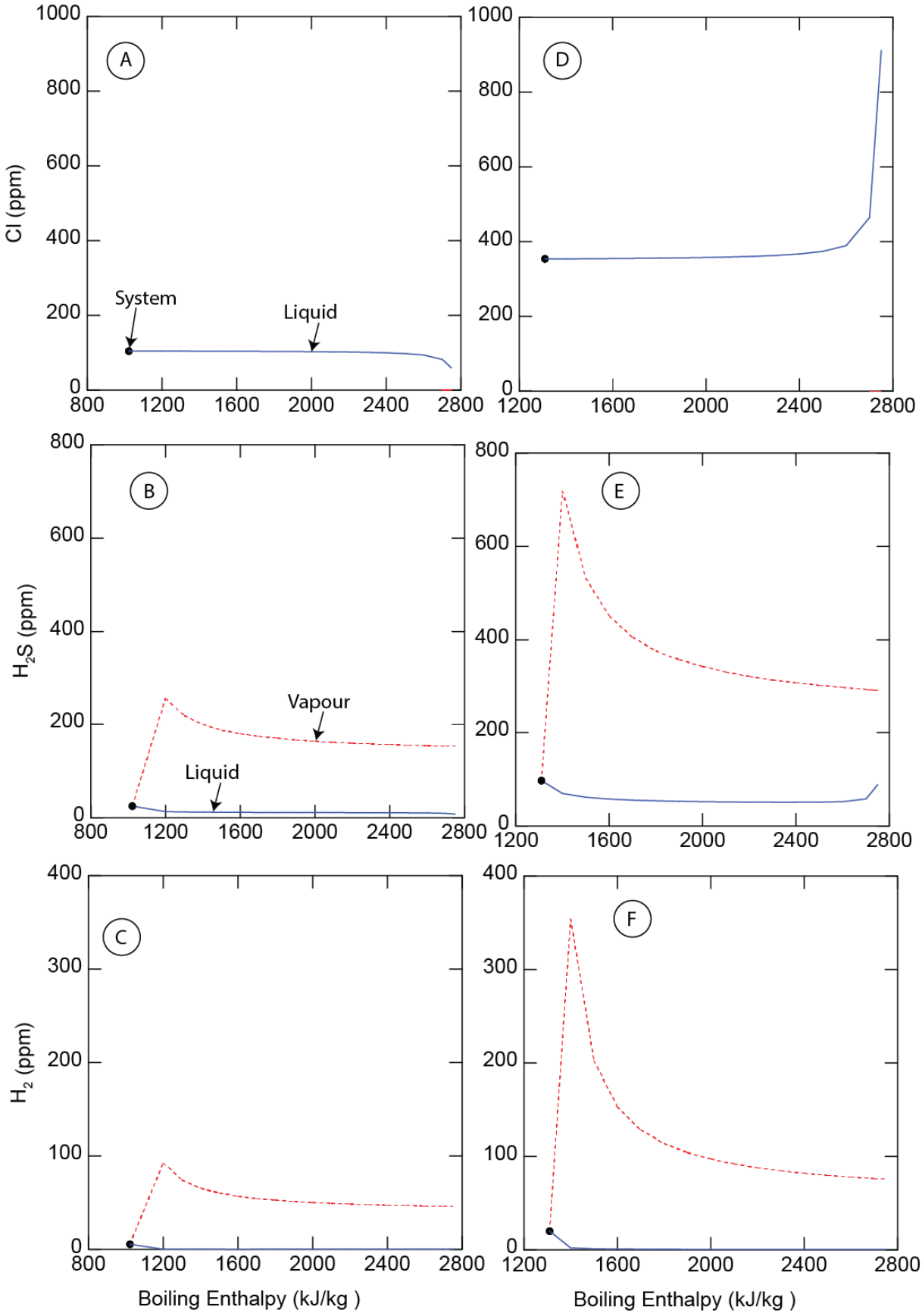

FIGURE 12: Example of major element and gas concentration changes (Cl, H_2S and H_2) in liquid and vapour phases upon isobaric boiling of reservoir fluids

Based on these simple modelling examples it can be concluded that boiling and evaporation may cause fractions of δD and $\delta^{18}O$ from the reservoir to the sampling conditions of >30‰ and >5‰ (Figure 13). In contrast, reservoir vapour formation due to addition of heat by, for example a magmatic intrusion, has less effects on the δD and $\delta^{18}O$ composition or <3‰ and <1‰, respectively, when temperatures are >200°C. For comparison, the range of measured values in this study were much less than the maximum effects of boiling or ~17‰ and ~4‰ for δD and $\delta^{18}O$, respectively, when considering both liquid and vapour phases. It is therefore clear that in order to assess proper reservoir δD and $\delta^{18}O$ and trace the origin of the water, an appropriate sampling and analysis strategy must be applied that includes: (1) sampling of liquid and vapour phases at the same temperature and pressure conditions from a Webre separator, (2) sampling at relatively high temperatures and pressures to minimize the effects of boiling on δD and $\delta^{18}O$ fractionation; and (3) sampling and analysis for δD and $\delta^{18}O$ of both vapour and liquid phase and not target one phase (e.g. liquid phase only) in the sampling. In contrast, sampling and analysis of δD and $\delta^{18}O$ for a single phase or sampling of the vapour phase from Webre separator and a liquid phase from a weirbox introduces additional uncertainties of a reconstructed reservoir or system δD and $\delta^{18}O$ values.

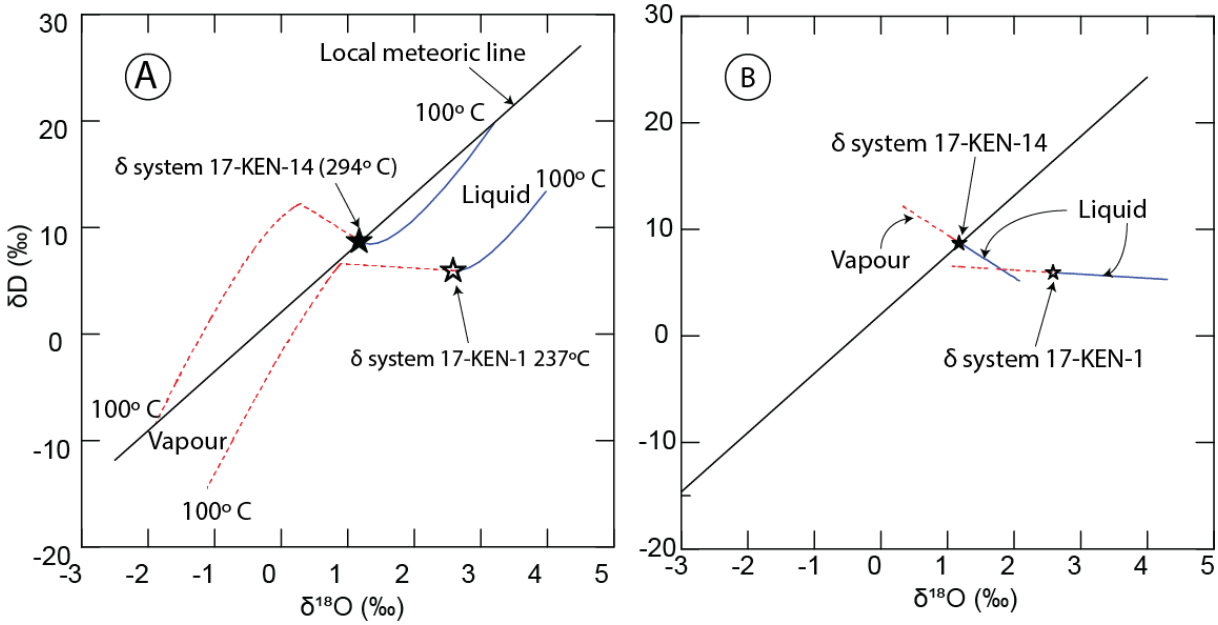

FIGURE 13. Isotope evolution upon (A) adiabatic and (B) isobaric boiling for 17-KEN-1 and 17-KEN-14 plotted against the local meteoric line; Kenyan Rift Meteoric Line (KRML), $\delta^2H=5.56\delta^{18}O+2.04$, from Allen et al. (1989)

6.2 Reservoir fluid composition and δD and $\delta^{18}O$ systematics

The reservoir fluid chemical and isotope compositions were further calculated from samples collected from the wellheads using a Webre separator. Two approaches were used for the calculations, one assuming the reservoir to be liquid only and that the reservoir enthalpy corresponded to the liquid enthalpy at reservoir temperature, and the latter using the measured discharge enthalpy. In both cases boiling from the reservoir to the sampling temperatures and pressures was assumed to be adiabatic. The calculations were carried out with the aid of the WATCH program (Bjarnason, 2010) and IsoGEM (Stefánsson et al., in prep.).

The reservoir chemical composition reconstructed from the two-phase fluid samples using liquid enthalpy at the temperature of the reservoir (T^{res}) (calculated enthalpy) is shown in Table 4 and the chemical composition obtained using measured enthalpy is given in Tables 5a and 5b. The aquifer isotope composition of reservoir fluid obtained using calculated enthalpy from the vapour and the liquid phase samples is shown in Table 6 while that obtained using measured enthalpy is shown in Table 7. Figure 14 shows the results of the aquifer isotope composition using the two enthalpies.

TABLE 4: Aquifer fluid composition at calculated enthalpy. Concentrations are in ppm

Sample #	Well #	T^{Qtz}	T^{NaK*}	pH	B	SiO_2	Na	K	Mg	Ca	F	Cl	SO_4	Al	Fe	CO_2	H_2S	H_2	CH_4	N_2
17-KEN-1	OW-41	237	302	6.50		408	167	41.9	0.026	0.44	64.4	105	4.13	1.82	0.005	825	24.6	5.49	0.180	2.41
17-KEN-2	OW-725	233	223	6.58	2.10	393	390	47.6	0.022	0.58	35.9	251	0.00	1.21	0.022	2452	119	11.5	1.92	6.71
17-KEN-4	OW-37A	260	310	7.62	6.55	540	841	234	0.012	0.25	139	1050	89.3	0.50	0.014	543	67.5	4.20	0.810	21.1
17-KEN-5	OW-44A	263	318	6.77		526	515	153	0.019	0.59	64.0	745	36.1	1.02	0.013	867	24.0	6.98	0.990	7.46
17-KEN-6	OW-907A	262	257	6.80	1.29	521	258	43.3	0.020	0.39	40.9	102	14.6	1.13	0.018	4750	15.3	7.58	4.63	7.27
17-KEN-7	OW-910	271	280	7.50	2.57	575	336	69.2	0.007	0.18	107	200	7.65	0.68	0.021	1260	33.1	8.55	1.23	4.24
17-KEN-8	OW-35	274	287	6.89	8.25	573	463	102	0.021	0.37	68.9	512	19.3	1.54	0.015	3770	1.28	21.8	1.99	7.66
17-KEN-9	OW-910B	261	266	7.45	1.48	530	329	59.5	0.020	0.37	47.4	114	12.9	1.19	0.023	1840	67.8	6.08	1.93	6.43
17-KEN-12	OW-714	255	248	6.93	2.06	594	402	62.3	0.019	0.40	56.8	354	24.6	1.13	0.016	2242	141	9.57	2.00	8.68
17-KEN-13	OW-916A	276	284	7.26	2.86	589	428	91.5	0.020	0.44	180	216	5.49	0.93	0.020	2075	30.8	11.8	5.08	4.40
17-KEN-14	OW-732	294	301	7.19	2.56	655	313	77.3	0.023	0.56	38.8	354	4.48	1.22	0.038	2647	97.0	20.1	4.40	17.2
17-KEN-15	OW-42	258	276	6.33		503	127	25.0	0.024	0.73	28.1	168	7.97	3.43	0.212	619	24.5	2.99	0.220	3.21
17-KEN-16	OW-720	235	215	7.02	1.84	412	368	42.8	0.019	0.50	51.9	219	54.0	0.86	0.021	980	37.9	5.88	0.930	6.26
17-KEN-17	OW-904	253	252	7.02	1.29	483	380	60.8	0.025	0.46	44.2	104	10.9	1.02	0.023	3740	3.54	10.2	8.72	6.44

* Arnórsson et al., (1983)

TABLE 5a: Aquifer fluid composition calculated from measured enthalpy. Shown is the liquid phase composition. Concentrations are in ppm

																	Liquid phase (ppm)			
Sample #	Well #	T^{Qtz}	T^{NaK}	pH	B	SiO_2	Na	K	Mg	Ca	F	Cl	SO_4	Al	Fe	CO_2	H_2S	H_2	CH_4	N_2
17-KEN-1	OW-41	207	303	7.39		300	123	30.8	0.019	0.320	47.3	76.7	3.03	1.34	0.003	50.8	7.23	0.020	0.000	0.010
17-KEN-2	OW-725	222	224	7.80	2.05	384	380	46.4	0.021	0.560	35.0	245	0.00	1.18	0.211	261	69.6	0.060	0.010	0.020
17-KEN-4	OW-37A	244	311	8.18	6.70	552	859	239	0.012	0.250	142	1070	91.2	0.507	0.014	121	69.6	0.040	0.010	0.140
17-KEN-5	OW-44A	245	319	7.53		464	454	135	0.017	0.520	56.4	657	31.9	0.898	0.012	63.7	6.52	0.060	0.010	0.040
17-KEN-6	OW-907A	256	258	7.83	1.31	527	261	43.8	0.020	0.400	41.4	103	14.7	1.14	0.018	660	2.81	0.110	0.070	0.080
17-KEN-7	OW-910	259	282	8.21	2.66	595	348	71.7	0.007	0.190	111	207	7.93	0.709	0.022	288	30.4	0.120	0.020	0.050
17-KEN-8	OW-35	268	287	7.83	8.36	581	470	103	0.021	0.380	79.9	519	19.5	1.56	0.016	492	0.60	0.350	0.030	0.100
17-KEN-9	OW-910B	245	267	8.27	1.54	554	344	62.1	0.020	0.390	49.5	119	13.4	1.23	0.024	513	52.6	0.070	0.020	0.050
17-KEN-12	OW-714	246	249	8.10	2.08	499	408	62.9	0.019	0.400	57.3	353	24.9	1.14	0.015	304	82.6	0.090	0.020	0.060
17-KEN-13	OW-916A	265	285	8.10	2.93	603	437	93.6	0.020	0.450	184	221	5.62	0.952	0.020	325	20.0	0.160	0.070	0.050
17-KEN-14	OW-732	290	302	7.89	2.60	666	318	78.5	0.023	0.570	39.4	360	4.55	1.24	0.039	456	53.7	0.640	0.150	0.450
17-KEN-15	OW-42	236	276	6.93		407	103	20.3	0.020	0.590	22.7	136	6.45	2.77	0.172	24.0	4.22	0.020	0.000	0.020
17-KEN-16	OW-720	219	217	8.06	1.81	401	362	42.1	0.019	0.490	51.1	216	53.2	0.848	0.021	179	24.6	0.030	0.000	0.020
17-KEN-17	OW-904	242	254	8.03	1.31	495	389	62.4	0.026	0.470	45.3	106	11.2	1.04	0.023	755	2.63	0.120	0.100	0.050

TABLE 5b: Aquifer fluid composition calculated from measured enthalpy

Vapour phase (mmol/kg)						
Sample #	**Well #**	**CO_2**	**H_2S**	**H_2**	**CH_4**	**N_2**
17-KEN-1	OW-41	145	4.46	22.8	0.091	0.717
17-KEN-2	OW-725	341	16.3	37.7	0.790	1.58
17-KEN-4	OW-37A	72.0	6.52	13.0	0.312	4.66
17-KEN-5	OW-44A	104	2.40	19.2	0.338	1.46
17-KEN-6	OW-907A	721	0.627	26.2	2.00	1.80
17-KEN-7	OW-910	173	3.06	28.5	0.511	1.01
17-KEN-8	OW-35	476	0.138	61.4	0.702	1.54
17-KEN-9	OW-910B	275	4.42	23.4	0.926	1.77
17-KEN-12	OW-714	296	14.4	29.2	0.764	1.89
17-KEN-13	OW-916A	226	2.57	30.5	1.64	0.815
17-KEN-14	OW-732	336	11.4	60.3	1.65	3.68
17-KEN-15	OW-42	72.2	4.25	9.02	0.081	0.691
17-KEN-16	OW-720	147	3.38	20.0	0.394	1.52
17-KEN-17	OW-904	631	0.371	42.6	4.54	1.92

TABLE 6: Reservoir fluid isotope composition calculated using liquid enthalpy at quartz geothermometry temperature

Sample #	**Well#**	**Reservoir T^{Qtz} (°C)**	**δD ‰**	**$\delta^{18}O$ ‰**
17-KEN-1	OW-41	237	5.9	2.58
17-KEN-2	OW-725	233	12.8	1.60
17-KEN-3	OW-735	260	6.4	0.44
17-KEN-4	OW-37A	263	0.1	0.39
17-KEN-5	OW-44A	262	1.8	1.75
17-KEN-6	OW-907A	271	8.6	1.14
17-KEN-7	OW-910	274	8.6	1.95
17-KEN-8	OW-35	261	2.2	1.07
17-KEN-9	OW-910B	255	6.1	1.42
17-KEN-10	OW-909	276	8.3	1.88
17-KEN-12	OW-714	294	10.9	1.37
17-KEN-13	OW-916A	258	14.6	2.61
17-KEN-14	OW-732	235	8.7	1.19
17-KEN-15	OW-42	253	10.5	2.35
17-KEN-16	OW-720	237	11.5	0.98
17-KEN-17	OW-904	233	11.8	1.70

TABLE 7: Aquifer fluid isotope composition calculated using measured enthalpy

Sample #	**Well#**	**Reservoir T^{qtz} [°C]**	**h^s [kJ/kg]**	**δD [‰]**	**$\delta^{18}O$ [‰]**
17-KEN-1	OW-41	207	2747	6.2	1.33
17-KEN-2	OW-725	222	2180	7.8	-0.10
17-KEN-3	OW-735		2240	3.9	-0.59
17-KEN-4	OW-37A	244	2670	-2.1	-0.84
17-KEN-5	OW-44A	245	1786	-0.1	0.00
17-KEN-6	OW-907A	256	2049	7.8	0.46
17-KEN-7	OW-910	259	2301	7.8	1.03
17-KEN-8	OW-35	268	1756	0.1	0.30
17-KEN-9	OW-910B	245	1754	5.6	0.79
17-KEN-10	OW-909		2144	6.7	1.14
17-KEN-12	OW-714	246	1725	8.2	0.58
17-KEN-13	OW-916A	265	2718	11.3	1.40
17-KEN-14	OW-732	290	2287	7.5	0.71
17-KEN-15	OW-42	236	1568	7.5	0.73
17-KEN-16	OW-720	219	2747	6.7	-0.63
17-KEN-17	OW-904	242	2180	10.3	1.07

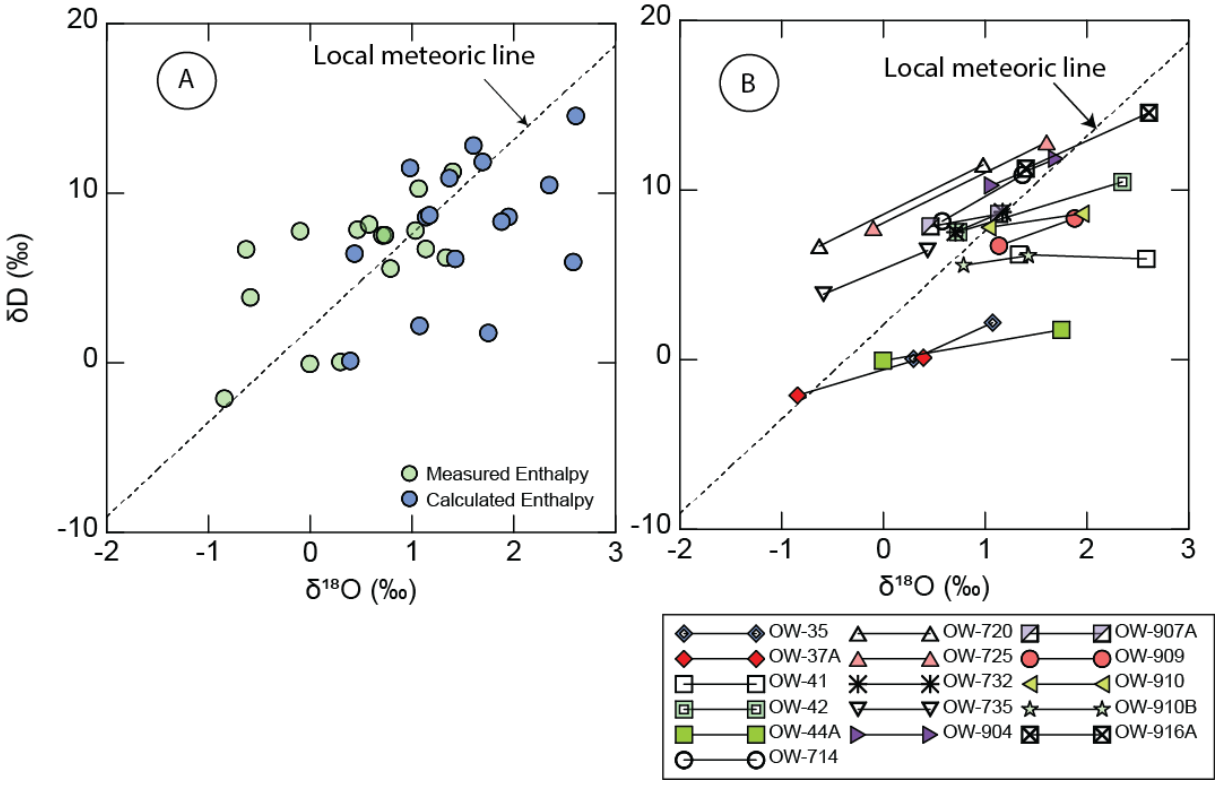

FIGURE 14: (A) Reservoir isotope composition of Olkaria fluid. (B) Comparison of the results of the two models used to reconstruct reservoir isotope composition of the wells sampled

The pH of the fluids assuming liquid only reservoir was 6.34-7.65, due to addition of CO_2 and H_2S back into the fluid compared to a pH of up to 10 for the surface samples. The non-volatile components displayed lower concentrations in the reservoir fluid compared to sampling compositions. Water (H_2O) was the dominant component of the fluid, making up 99.73-99.92 mol%. SiO_2, Na and Cl were in the range of 390-659, 128-847 and 103-1055 ppm, respectively. Carbon dioxide concentrations ranged from 530 to 4700 ppm. In contrast, the reservoir fluid composition calculated using the measured enthalpy resulted in two phase (vapour and liquid) reservoir fluid. Most of the volatile components (major gases) were calculated to be present in the reservoir vapour phase including CO_2 and H_2S that resulted in the pH of the liquid phase to be higher than when assuming liquid only reservoir, with values between 6.9 and 8.3. Water was the dominant component in the liquid and vapour phases with concentrations of 99.8-99.9 and 98.7-99.9 mol%, respectively. Silica, Na and Cl in the liquid phase were in the range of 300-670, 100-860 and 80-1100 ppm, respectively.

The reservoir or system isotope composition obtained using calculated enthalpy was in the range of +0.1 to +14.6‰ and +0.39 to +2.61‰ for δD and $\delta^{18}O$, respectively. Those from calculations using measured enthalpy of the wells were in the range of -2.1 to +11.3‰ and +0.84 to +1.40‰ for δD and $\delta^{18}O$, respectively. The isotope composition of the reservoir fluids are shown in Figure 14. As observed, a considerable scatter is observed of the data depending on what method was applied for the calculation of reservoir δD and $\delta^{18}O$ values in addition to the spread of the data. These differences between the two models are in the range of 1-4‰ and 1-3‰ for δD and $\delta^{18}O$, respectively, exceeding largely the analytical errors for δD and $\delta^{18}O$ of <1‰ and <0.1‰, respectively.

6.3 Origin of geothermal water of the Olkaria geothermal system

It is generally accepted that the majority of water in active geothermal systems are of meteoric or seawater origin with insignificant contribution from magmatic sources (e.g., Craig, 1963, 1961; Árnason, 1977; Truesdell and Hulston, 1980). Upon water-rock interaction, the $\delta^{18}O$ of the water tends to shift to higher values whereas δD ratios are mainly unaffected by water-rock reactions.

The local rainwater around Olkaria geothermal system varies considerably in δD and $\delta^{18}O$ composition. The δD and $\delta^{18}O$ values of rainwater in the rift valley vary across and along the rift valley due to changes in altitude. The floor of rift is the highest in elevation in the central part (>2000 m asl) where the Olkaria Geothermal system is located and falls gradually towards north (~900 m asl in Turkana) and to the south (~600 m asl at Lake Magadi). Across the rift valley where Olkaria is located, the eastern flank is up to 3000 m asl while the west flank is at 2600 m asl. Moreover, rain water falling in the rift valley is subject to evaporation and each rain storm may have a different isotope composition in the same area (Allen et al., 1989). The δD value of the rain that falls on the rift valley varies from -64‰ to +20‰ for δD while $\delta^{18}O$ varies from -10‰ to +5.4 ‰ (Figure 15). Within the Olkaria geothermal area, the δD and $\delta^{18}O$ ratios of precipitation are +6 to +19‰ and -1.6 and +1.4‰, respectively (Ojiambo et al., 2001). The rain that falls in the area at altitudes above 1800 m asl is of the range -64‰ to +5‰ and -10‰ to -0.2‰ for δD and $\delta^{18}O$, respectively. Streams and rivers draining into the catchment area of Naivasha have isotope values in the range of -62‰ to -5‰ and -9‰ to -0.1‰ for δD and $\delta^{18}O$, respectively. Ground waters from non-thermal water wells are in the range of -35‰ to +32‰ and -5.3‰ to +5.6‰ for δD and $\delta^{18}O$, respectively. The enriched values for non-thermal water wells are from wells drilled near Lake Naivasha, which has an isotope composition of ~+35 ‰ δD and ~ +7 ‰ $\delta^{18}O$ and may be drawing water from the lake. Some parts of the lake are isolated from the main lake, e.g. Oloiden bay, and have a local isotope enrichment with isotope values of 60‰ δD and 10‰ $\delta^{18}O$.

The δD and $\delta^{18}O$ isotope composition measured in vapour and liquid discharged from Olkaria, sampled at variable temperature and pressure conditions and using variable methods are compared with local rain, surface, non-thermal ground and Lake Naivasha

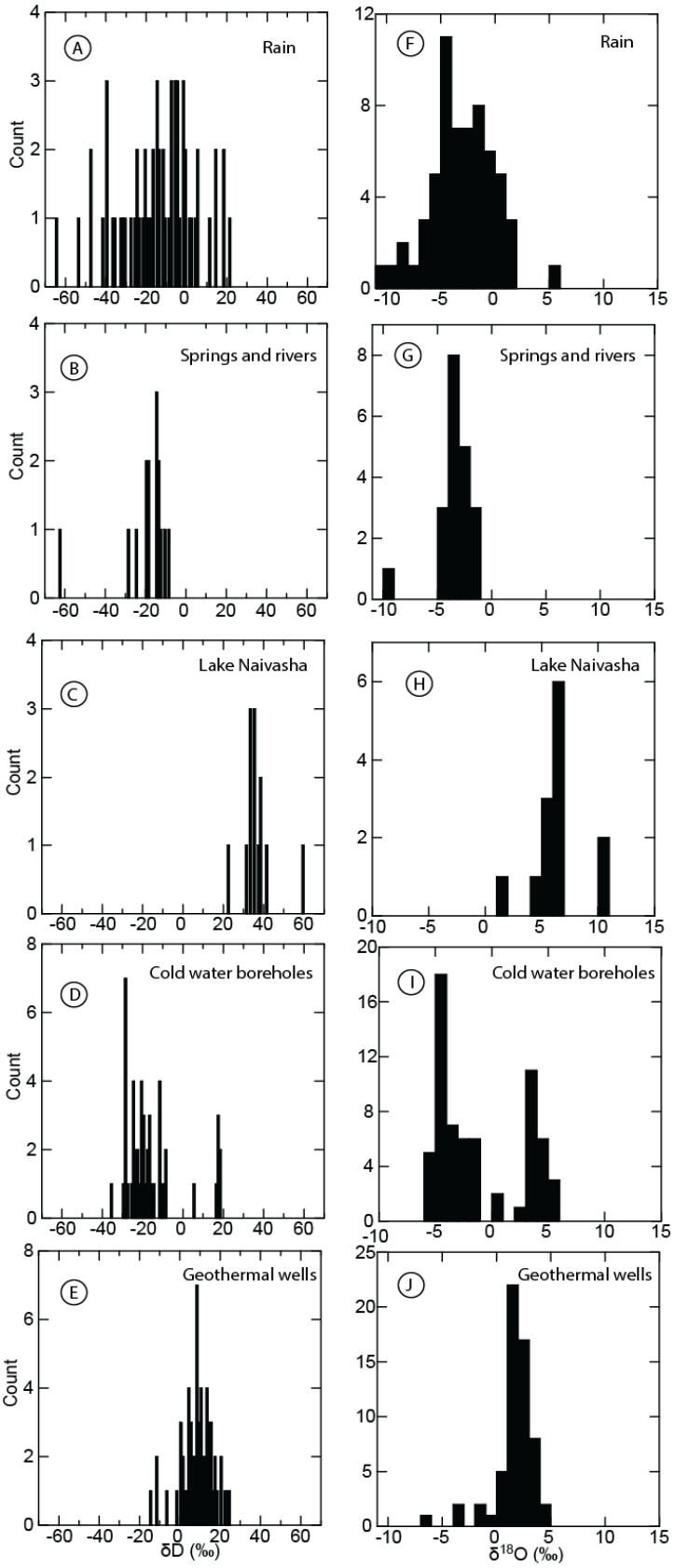

FIGURE 15: A comparison of δD and $\delta^{18}O$ of rainfall, rivers, springs, cold-wells, Lake Naivasha and Olkaria geothermal wells; data from this study and previous studies (Allen et al., 1989; Allen and Darling, 1987; Karingithi, 2000; Ojiambo et al., 2001; Sekento, 2012; Sveinbjörnsdóttir, 1988)

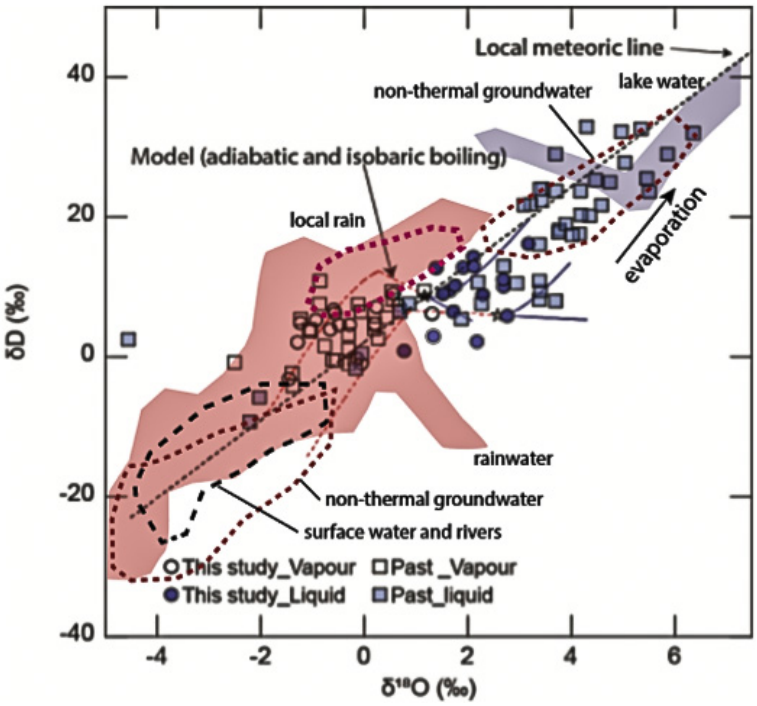

FIGURE 16: The δD and $\delta^{18}O$ relationship for measured geothermal discharge fluids; also shown are the ranges of values for local rainwater, non-thermal groundwater, surface and rivers and lake water. For references see Figure 15

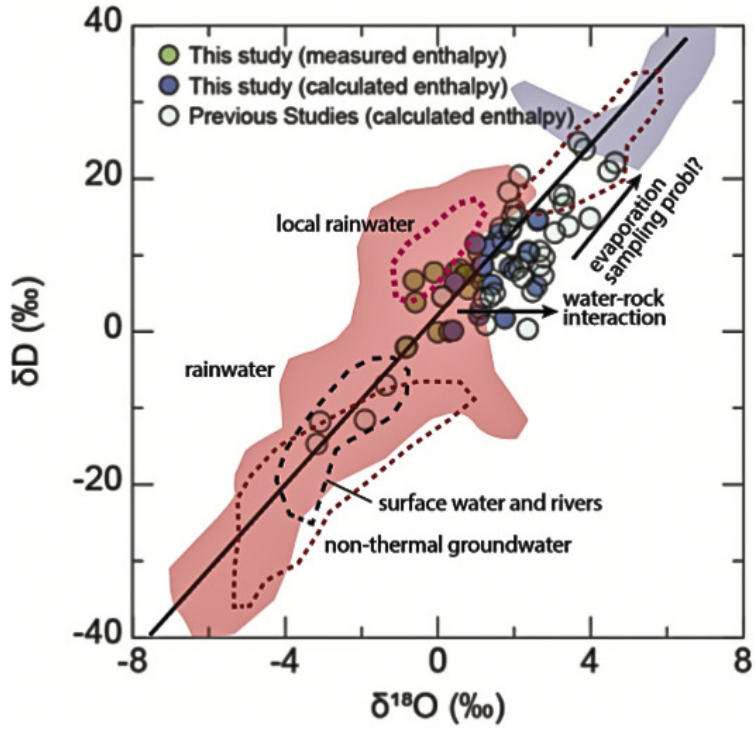

FIGURE 17: The δD and $\delta^{18}O$ relationship for reservoir geothermal fluids; also shown are the trends for evaporation and progressive water-rock interaction. Also shown are ranges of values for local rainwater, non-thermal groundwater, surface and rivers and lake water. For references, see Figure 15

water in Figure 16. Also shown are the variations related to adiabatic boiling from the reservoir to surface temperatures. Previous reported isotope values are also shown. As observed, a large scatter is observed in the data making conclusive estimations of the water sources only based on δD and $\delta^{18}O$ composition somewhat difficult. In Figure 17, the various non-thermal waters are compared with the calculated reservoir fluid δD and $\delta^{18}O$ isotope compositions. Inspection of Figure 17 suggests two points that need to be addressed before the water sources at Olkaria are assessed. Firstly, the dataset obtained in this study displays smaller δD and $\delta^{18}O$ variations than the previous dataset. For the previous datasets, samples were generally collected of the liquid phase at the weirbox and are a subject of considerable isotope fractionation due to boiling and evaporation. Elevated δD and $\delta^{18}O$ values may, therefore, not be representative in all cases of discharge and reservoir fluids. Secondly, most geothermal reservoir fluids are shifted for $\delta^{18}O$ relative to the local meteoric line. This is suggested to indicate progressive water-rock interaction (e.g., Stefánsson et al., 2017).

According to the present dataset, the δD values of the reservoir geothermal fluids are between -2.1 to +14.6‰. These values are similar to the local precipitation around Olkaria geothermal area (with rain water δD values up to +19‰). Previously, however, it has been suggested (Owens et al., 2015; Ojiambo and Lyons 1993) that 30-70% of the geothermal waters at Olkaria may originate from Lake Naivasha due to elevated δD. This may in fact be in error due to sampling issues and related boiling and evaporation. The contribution of the Lake Naivasha water is determined by first identifying an end member meteoric source component and then mixing it with

lake water to arrive at the range of isotope composition observed in the Olkaria geothermal system. The selection of this starting meteoric end member mixing with the Lake Naivasha water may not be a straightforward one as the isotope composition of rainwater in the rift valley is variable and even the local rainwater is similar in isotope composition with the reservoir fluid.

6.4 Conceptual hydrological model of Olkaria based on δD and $\delta^{18}O$

The geothermal reservoir fluids at Olkaria are predominantly meteoric in origin in line with previous studies (e.g., Ojiambo and Lyons, 1993; Karingithi 2000; Nkapiani, 2014; Owens et al., 2015). The meteoric water probably enters the system from all directions and locally through faults and fractures (Figure 18). Upon water-rock interaction, the geothermal waters are further modified, with a shift of $\delta^{18}O$ to higher values.

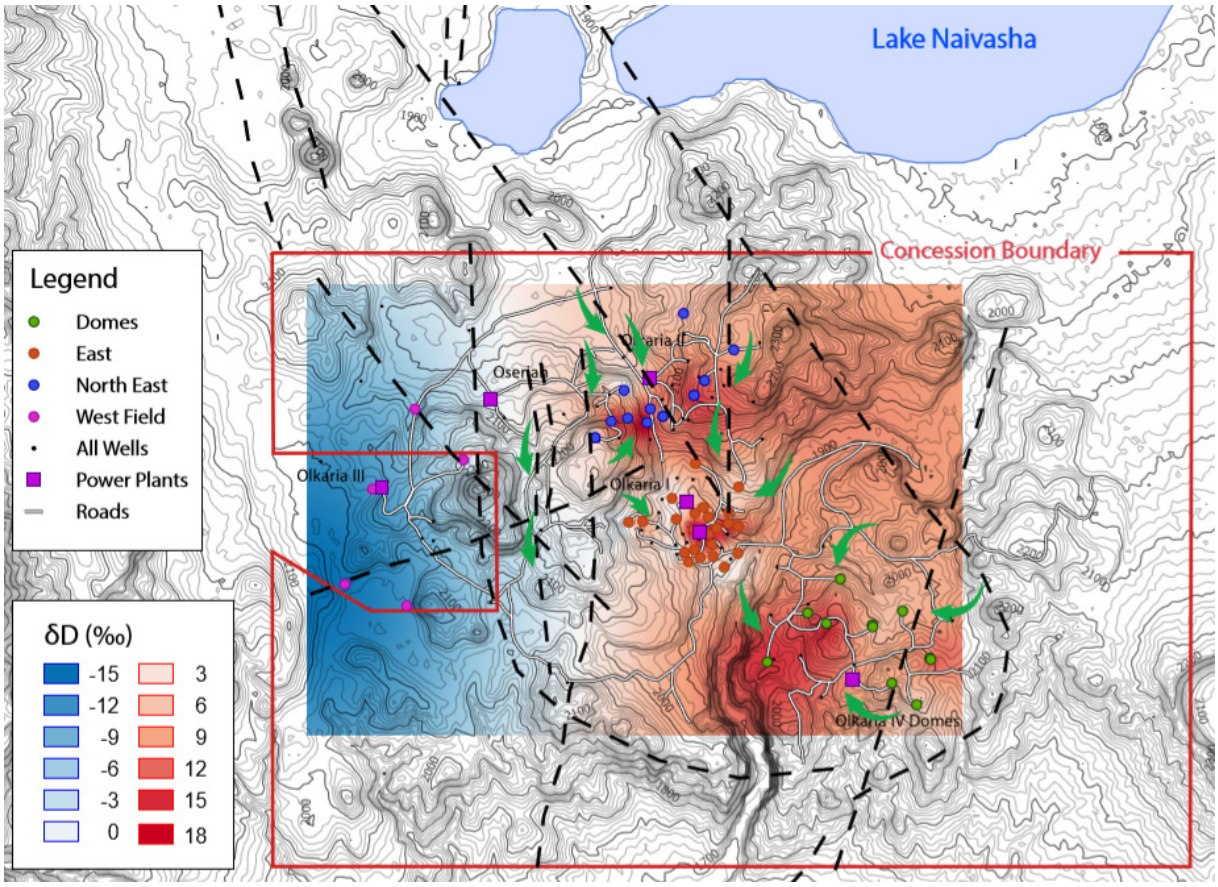

FIGURE 18: The distribution of δD of the reservoir geothermal fluids at Olkaria. It is concluded that majority of the waters are local precipitation within the area and surrounding mountains

According to Meins (2013), the average precipitation occurring in Naivasha catchment area is 650 mm/yr. around Lake Naivasha and 1250-1500 mm/yr. in the Mau (western flank) and Aberdare range (eastern flank).

The total mass flow from Olkaria geothermal field with the current electricity generation is 10,270 tons/hr (East: 2870, Northeast: 1472, Domes: 2729 and Olkaria West: 3195) (KenGen, internal data; Owens et al., 2015). This translates to a total mass flow of 9.0×10^7 tons/yr. Approximately 60% of this mass is injected back into the geothermal system. Assuming all rainwater in the area to enter the ground and accounting for the additional 40% of water recharging the system, a surface area of ~25-55 km^2 is needed. For comparison, the concession boundary of Olkaria geothermal field (marked red in Figure 18) is 204 km^2. Therefore, it is concluded that the geothermal water at Olkaria must be predominantly close

to local precipitation, in line with water budget and isotope composition of the discharge fluids and local precipitation.

The total ground water seepage from Lake Naivasha however, has been estimated to be 6.95×10^7 tons/yr. (Hogeboom et al., 2015). The total of seepage estimated to flow to the south is approximately 73% or 4.9×10^7 tons. Allen et al., (1989) suggested that less than 25% of this southerly flow might be contributing to a deeper flow to the depths of the geothermal system. It can be concluded that geothermal fluids at Olkaria might have a minor contribution originating from Lake Naivasha but, however, minor this contribution is, the lake water component may not be effectively traced using stable isotopes of water alone and other tracers can be explored.

7. CONCLUSION

The δD and $\delta^{18}O$ systematics and the origin of geothermal fluids at Olkaria, Kenya were studied The reservoir δD and $\delta^{18}O$ ratios, calculated from data from well discharge, ranged from -2.1 to +14.6‰ and -0.84 to +2.61‰, respectively. According to boiling modelling, large δD and $\delta^{18}O$ fractionations can occur from the reservoir to sampling at surface, and these changes exceed the range of observed δD and $\delta^{18}O$ variability for fluids at Olkaria. Accurate reconstruction of the reservoir and source δD and $\delta^{18}O$ requires, therefore, careful sampling, analysis and geochemical and isotope modelling. Based on the composition of the reservoir δD and $\delta^{18}O$ and the local rainwater, surface water, lake water and non-thermal groundwater, it is concluded that the geothermal reservoir fluids at Olkaria are predominantly local meteoric water from within the area and surrounding flanks of the rift valley.

REFERENCES

Allen, D.J., and Darling, W.G., 1987: *Kenya Rift Valley geothermal project: Hydrogeology progress report.* British Geological Survey, Wallingford, U.K, report No. WD/OS/87/16, 65 pp.

Allen, D., Darling, G., and Burgess, W., 1989. *Geothermics and hydrogeology of the southern part of the Kenya Rift Valley with emphasis on the Magadi-Nakuru area.* British Geological Survey, Nottingham, UK, report No. SD/89/001, 197 pp.

Árnason, B., 1977: Hot groundwater systems in Iceland traced by Deuterium. *Hydrology Research, 8*, 93–102.

Arnórsson, S., Bjarnason, J., Giroud, N., Gunnarsson, I., and Stefánsson, A., 2006: Sampling and analysis of geothermal fluids. *Geofluids, 6*, 203–216.

Arnórsson, S., Gunnlaugsson, E., and Svavarsson, H., 1983: The chemistry of geothermal waters in Iceland III. Chemical geothermometry in geothermal investigations. *Geochim. Cosmochim. Acta, 47*, 567-577.

Arnórsson, S., Sigurdsson, S., and Svavarsson, H., 1982: The chemistry of geothermal waters in Iceland. I. Calculation of aqueous speciation from 0° to 370°C. *Geochim. Cosmochim. Acta, 46*, 1513–1532.

Arnórsson, S., Stefánsson, A., and Bjarnason, J.Ö., 2007: Fluid-fluid interactions in geothermal systems. *Rev. Mineral. Geochem., 65*, 259–312.

Axelsson, G., Arnaldsson, A., Ármannsson, H., Árnason, K., Einarsson, G., Franzson, H., Fridriksson, Th., Gudmundsson, G., Gylfadóttir, S.S., and Halldórsdóttir, S., 2013: Updated conceptual model and capacity estimates for the Greater Olkaria geothermal system, Kenya. *Proceedings of the 38th Workshop on Geothermal Reservoir Engineering, Stanford University, Stanford, Ca,* 9 pp.

Axelsson, G., Guðmundsson, G., Arnaldsson, A., Ármannsson, H., Árnason, K., Einarsson, G., Franzson, H., Halldórsdóttir, S., Hersir, G.P., Níelsson, S., Kamunya, K., Ouma, P., Okoo, J.A., Rop, E., Omiti, A., Wamalwa, R., Óskarsson, F., Saitet, D., and Mwarania, F., 2017: Revision of the conceptual model for the Olkaria geothermal system, Kenya. *Proceedings of the 42nd Workshop on Geothermal Reservoir Engineering, Stanford University, Stanford, CA,* 19 pp.

Baker, B.H., 1986: Tectonics and volcanism of the southern Kenya Rift Valley and its influence on rift sedimentation. Geological Society, London, Special Publications, 25, 45–57

Baker, B.H., Mohr, P.A., and Williams, L.A.J., 1972: Geology of the Eastern Rift System of Africa, *Geological Society of America, Special Papers,* 1–68.

Baker, B.H., Williams, L.A.J., Miller, J.A., and Fitch, F.J., 1971: Sequence and geochronology of the Kenya rift volcanics. *Tectonophysics, 11*, 191–215.

Bjarnason, J.Ö., 2010: The speciation program WATCH, version 2.4. Orkustofnun, Reykjavík.

Chorowicz, J., 2005: The East African rift system. *J. Afr. Earth Sci*., *43*, 379–410.

Clarke, M., Allen, D., Darling, G., and Woodhall, D., 1990: *Geological, volcanological and hydrogeological controls on the occurrence of geothermal activity in the area surrounding Lake Naivasha, Kenya*: *with coloured 1:250 000 geological maps.* Ministry of Energy, Nairobi, 138 pp.

Craig, H., 1961: Isotopic variations in meteoric waters. *Science, 133, 1702-1703.*

Craig, H., 1963: The isotopic geochemistry of water and carbon in geothermal areas. In: Tongiorgi, E. (ed.), *Nuclear geology on geothermal areas*. Consiglio Nazionale delle Ricerche, Laboratorio di Geologia Nucleare, Pisa, 17-53.

Davies, G.R., and Macdonald, R., 1987: Crustal influences in the petrogenesis of the Naivasha basalt – comendite complex: combined trace element and Sr-Nd-Pb isotope constraints. *J. Petrol., 28*, 1009–1031.

Fournier, R.O., and Potter, R.W. II, 1982: A revised and expanded silica (quartz) geothermometer. *Geoth. Res. Council, Bull.,11-10*, 3-12.

Hogeboom, R.H.J., van Oel, P.R., Krol, M.S., and Booij, M.J., 2015: Modelling the influence of groundwater abstractions on the water level of Lake Naivasha, Kenya under data-scarce conditions. *Water Resources Management, 29*, 4447–4463

Horita, J., and Wesolowski, D.J., 1994: Liquid-vapour fractionation of oxygen and hydrogen isotopes of water from the freezing to the critical temperature. *Geochim. Cosmochim. Acta, 58*, 3425–3437.

Karingithi, C.W., 2000: Geochemical characteristics of the Greater Olkaria geothermal field, Kenya. Report 9 in: *Geothermal training in Iceland 1998.* UNU-GTP, Iceland, 165-188.

Karingithi, C.W., 2002: *Hydrothermal mineral buffers controlling reactive gases concentration in the Greater Olkaria geothermal system, Kenya*. University of Iceland, MSc thesis, UNU-GTP, Iceland report 2, 51 pp.

Karingithi, C.W., Arnórsson, S., and Grönvold, K., 2010: Processes controlling aquifer fluid compositions in the Olkaria geothermal system, Kenya. *J. Volc. Geothermal Res., 196,* 57-76.

Lagat, J.K., 2004: *Geology, hydrothermal alteration and fluid inclusion studies of the Olkaria Domes geothermal field, Kenya.* University of Iceland, MSc thesis, UNU-GTP, Iceland, report 2, 71 p.

Macdonald, R., 1994: Petrological evidence regarding the evolution of the Kenya Rift Valley. Crustal and upper mantle structure of the Kenya Rift. *Tectonophysics, 236,* 373–390.

Macdonald, R., 2002: Magmatism of the Kenya Rift Valley: A review. *Earth Environ. Sci. Trans., R. Soc. Edinb. 93,* 239–253.

Macdonald, R., Belkin, H.E., Fitton, J.G., Rogers, N.W., Nejbert, K., Tindle, A.G., and Marshall, A.S., 2008: The roles of fractional crystallization, magma mixing, crystal mush remobilization and volatile-melt interactions in the genesis of a young basalt-peralkaline rhyolite suite, the Greater Olkaria volcanic complex, Kenya Rift valley. *J. Petrology, 49,* 1515-1547.

Macdonald, R., Davies, G.R., Bliss, C.M., Leat, P.T., Bailey, D.K., and Smith, R.L., 1987: Geochemistry of high-silica peralkaline rhyolites, Naivasha, Kenya Rift Valley. *J. Petrol., 28,* 979-1008.

Macdonald, R., and Scaillet, B., 2006: The central Kenya peralkaline province: Insights into the evolution of peralkaline salic magmas. *Lithos, 91,* 59–73.

Macdonald, R., Williams, L. a. J., Gass, I.G., 1994: Tectonomagmatic evolution of the Kenya rift valley: some geological perspectives. *J. Geol. Soc. 151,* 879–888.

Macgregor, D., 2015: History of the development of the East African Rift System: A series of interpreted maps through time. *J. African Earth Sciences*, *101*, 232–252.

Meins F.M., 2013. *Evaluation of spatial scale alternatives for hydrological modelling of the Lake Naivasha basin, Kenya*. University of Twente, Enschede, MSc thesis, 155 pp.

Musonye, X.S., 2015: *Sub-surface petrochemistry, stratigraphy and hydrothermal alteration of the Domes area, Olkaria geothermal field, Kenya*. University of Iceland, MSc thesis, UNU-GTP, Iceland, Report 3, 100 pp.

Mwangi, D.W., 2012: Borehole geology and hydrothermal mineralisation of well OW–916, Olkaria Domes geothermal field, Naivasha, Kenya. Report 24 in: *Geothermal training in Iceland 2012*. UNU-GTP, Iceland, 541-571.

Naylor, W.I., 1972: *Geology of the Eburru and Olkaria prospects.* U.N. Geothermal Exploration Project, report.

Njathi, D.W., 2012: Borehole geology and hydrothermal mineralisation of well OW-911A, Olkaria Domes geothermal field, Central Kenya Rift Valley. Report 25 in: *Geothermal training in Iceland 2012*. UNU-GTP, Iceland, 573-600.

Nkapiani, M.N., 2014: Application of stable isotope geochemistry to tracing recharge and flow systems of fluids in the Olkaria geothermal field, Kenya. Report 24, in: *Geothermal training in Iceland 2014*. UNU-GTP, Iceland, 483–504.

Noble, J.W., and Ojiambo, B.S., 1975: Geothermal exploration in Kenya. *Proceedings of the 2nd United Nations Symposium on the Development and Use of Geothermal Resources*, *San Francisco, California* 189–204.

Ofwona, C.O., 2002: *A reservoir study of Olkaria East geothermal system, Kenya*. University of Iceland, MSc thesis, UNU-GTP, Iceland, report 1, 74 pp.

Ojiambo, B.S., and Lyons, W.B., 1993: Stable isotope composition of Olkaria geothermal fluids, Kenya. *Geotherm. Resour. Counc., Trans., 17,* 149–153.

Ojiambo, B.S., Poreda, R.J., and Lyons, W.B., 2001: Ground water/surface water interactions in Lake Naivasha, Kenya, using $\delta^{18}O$, δD, and $^{3}H/^{3}He$ age-dating. *Groundwater, 39,* 526–533.

Okoo, J.A., 2013: Borehole geology and hydrothermal alteration mineralogy of well OW-39A, Olkaria geothermal project, Naivasha, Kenya. Report 24, in: *Geothermal training in Iceland 2013*. UNU-GTP, Iceland, 547–576

Otieno, V.O., 2016: *Borehole geology and sub-surface petrochemistry of the Domes area, Olkaria geothermal field, Kenya, in relation to well OW-922*. University of Iceland, MSc thesis, UNU-GTP, Iceland, Report 2, 84 pp.

Owens, L., Porras, E., Spielman, P., and Walsh, P., 2015: Updated geologic and geochemical assessment of the Olkaria III field following recent expansion to 110 MW. *Proceedings of the 40th Workshop on Geothermal Reservoir Engineering, Stanford University Stanford, CA,* 8 pp.

Pope, E.C., Bird, D.K., and Arnórsson, S., 2014: Stable isotopes of hydrothermal minerals as tracers for geothermal fluids in Iceland. *Geothermics, 49*, 99–110.

Pope, E.C., Bird, D.K., Arnórsson, S., and Giroud, N., 2016: Hydrogeology of the Krafla geothermal system, northeast Iceland. *Geofluids, 16*, 175–197.

Sekento, L.R., 2012: *Geochemical and isotopic study of the Menengai geothermal field, Kenya.* Report 31 in: *Geothermal training in Iceland in 2012*. UNU-GTP, Iceland, 769-792.

Simiyu, S.M., 2000: Geothermal reservoir characterization: Application of microseismicity and seismic wave properties at Olkaria, Kenya rift. *J. Geophysical Research, 105*, 13779–13795.

Stefánsson, A., Gunnarsson, I., and Giroud, N., 2007: New methods for the direct determination of dissolved inorganic, organic and total carbon in natural waters by Reagent-Free^{TM} Ion Chromatography and inductively coupled plasma atomic emission spectrometry. *Analytica Chimica Acta, 582,* 69–74.

Stefánsson, A., Hilton, D.R., Sveinbjörnsdóttir, Á.E., Torssander, P., Heinemeier, J., Barnes, J.D., Ono, S., Halldórsson, S.A., Fiebig, J., and Arnórsson, S., 2017: Isotope systematics of Icelandic thermal fluids. *J. Volcanology & Geothermal Research, 337,* 146–164.

Sveinbjörnsdóttir, Á.E., 1988: *Results of stable isotope measurements on samples from Olkaria and Eburru geothermal fields, Kenya*. Kenya Power Company, Ltd., Science Institute, University of Iceland, report.

Truesdell, A.H., and Hulston, J.R., 1980: Isotopic evidence on environments of geothermal systems. In: Fritz, P., and Fontes, J.C. (eds.), *A handbook of environmental, isotope geochemistry, Vol. 1, Ch. 5,* 179–226.